In-situ experimental investigations to study the impact of mechanical compression on the PEMFC - analysis of the global cell performance

El Mahdi Khetabi, Khadidja Bouziane, Xavier François, Remy Lachat, Yann Meyer, Denis Candusso

In-situ experimental investigations to study the impact of mechanical compression on the PEMFC - Analysis of the global cell performance

El Mahdi KHETABI[1], Khadidja BOUZIANE[1], Xavier FRANÇOIS[2], Remy LACHAT[3], Yann MEYER[4], Denis CANDUSSO[1]

[1] Univ. Paris Saclay, ENS Paris Saclay, Univ. Gustave Eiffel, SATIE, COSYS, FCLAB, 90010 Belfort Cedex, France.

[2] Univ. Bourgogne Franche-Comté, UTBM, FCLAB, 90010 Belfort Cedex, France.

[3] ICB, CNRS Univ. Bourgogne Franche-Comté, UTBM, 90000 Belfort, France.

[4] Univ. Savoie Mont Blanc, SYMME, 74000 Annecy, France.

Abstract:

An appropriate clamping pressure is required to ensure the gas-tight operation of a PEMFC assembly and to improve the contacts (i.e. mechanical, thermal, electrical) between its components. However, an excessive mechanical load may also worsen the cell performance, in particular through the reduction in the porosity and mass transport ability of the Gas Diffusion Layers. In this study, the effects of mechanical compression on the global performance of a 225 cm² PEMFC assembly are investigated by implementing cell voltage monitoring and polarisation curve measurements. The investigations are carried out with gradual increase / decrease and randomised load compression protocols applied using a specially designed mechanical compression unit. 12 levels of mechanical compression are considered, ranging from 0.35 to 2 MPa with steps of 0.15 MPa. The results of the characterisation techniques show that the PEMFC performance is improved at all tested operating conditions for mechanical compression up to 1.55 MPa. This finding is attributed to

the dominant reduction of the ohmic drop against the increase of the gas diffusion losses. It is also shown that compressing the PEMFC beyond 1.55 MPa would not lead to any further improvement of the global cell voltage output. This may even worsen the cell electrical characteristics by affecting its mass transport issues.

Keywords: PEMFC; Mechanical assembly; Clamping pressure; In-situ characterisation; Gas Diffusion Layer.

Highlights:

- The effects of clamping on the global performance of a 225 cm² PEMFC are studied.
- A cell compression unit is used to duplicate various mechanical loads (0.35 - 2 MPa).
- Investigations are done using cell voltage monitoring and polarisation curves.
- In all cases, the PEMFC performance is improved for mechanical load up to 1.55 MPa.
- The tests are correlated with ex-situ characterisations of GDL contact resistances.

1. Introduction and literature survey

Fuel Cell (FC) fed by hydrogen has been shown as a promising solution to decarbonise many sectors [1]. In the last few years, significant efforts have been made to commercialise PEMFC (Proton Exchange Membrane Fuel Cell) on a larger scale. With this relatively recent trend to deploy this technology in a wide range of applications, production needs to be shifted from small-scale manufacturing to more established industrial processes [2]. This trend led the research community to investigate different aspects related with the mechanics of FC stacks, from a few years ago [3-5] until more recently [6-10]. In fact, a PEMFC assembly is a multi-contact structure in which multi-physical phenomena are coupled. Interactions of these phenomena affect the performance of the FC. In this context, mechanical stress inside the PEMFC stack represents one of the main factors that affect the performance and durability of the FC [11-16].

In a PEMFC, two major types of compression mechanisms take place, the first is due to external forces (e.g. the applied compression during the assembly process), and the second is caused by internal forces that are generated inside the FC during its operation (e.g. membrane hydration / dehydration, temperature variation, freeze / thaw cycles). In both cases, components within the FC are subjected to compressive forces that may either improve or worsen the FC performance. FC stacks require mechanical compression during the assembly process to ensure both good electrical and thermal conductivities, between the stack components, and gas-tight operations. The clamping pressure influences not only the protonic and electronic conductivity but also the thickness and porosity of the Gas Diffusion Layers (GDLs). Recently, intensive research studies have focused on the GDLs due to the strong relation between their compressibility and the performance of the PEMFCs. The analysis of GDL compression is of paramount importance, as this cell component is responsible for

maintaining the functionality of the MEA by undergoing mechanical compression. The porous and fibrous structure of a GDL and its very small thickness compared to its other dimensions induce anisotropic, inhomogeneous and non-linear physical properties. In terms of its mechanical behaviour properties, this results in a non-linear stress-strain curve [15,5,6] that can possibly be linked to the global "assembly pressure vs. compression ratio" characteristic determined for the entire FC as the other cell components also play a role in the overall mechanical behaviour of the cell. The compression applied to the GDL has an effect on its dimensions and porosity, but also on its electrical properties. In fact, higher clamping pressure can lead to a decrease in GDL bulk resistance and in contact resistances with the other cell components. However, excessive compression forces and uneven distributions of compression in PEMFCs, particularly on the GDLs, can also have several detrimental impacts on the performance and durability of the cells: the decrease in the porosity of the GDL reduces the supply of reactant gases to the CLs (Catalyst Layers) and hinders excess water from being removed, the GDL structure can be compromised inducing a decrease of its mechanical strength.

Assembling a FC stack requires first an accurate control to ensure proper alignment of its individual components, then an appropriate assembly pressure is applied in order to achieve adequate contact between the FC components and to ensure gas-tight operation. In order to prevent hazardous situations, sealing gaskets are generally inserted between the Membrane Electrodes Assembly (MEA) and the Flow Field Plates (FFPs) (or BiPolar Plates - BPPs) to ensure that no gas leakage (between the FC and its external environment) occurs during the FC operations. Various investigations have been reported in the literature to assess compression characteristics during the assembly process and through various clamping mechanisms, either by simulations using numerical models [17-20] or experimental investigations using piezoresistive arrays [21,22] or pressure-sensitive thin films [19,20,23-

25]. However, each FC component has its unique characteristics, especially the GDLs. Thus, the assembly pressure depends on these characteristics, which makes it challenging to propose a recommended assembly pressure value for PEMFCs. Recent review articles have been devoted to PEMFC assembly and stack clamping methods, highlighting numerous technical and process design issues, as well as new scientific challenges [26-28].

In a previous review article [29], we have proposed a comprehensive overview of the studies that have focused on the relationship between mechanical compression, the effects of the generated stresses and the observed performance of a PEMFC operating in real life conditions (i.e. in-situ). The effects of GDL properties with respect to the applied mechanical compression and the operating conditions were investigated. Studies dealing with the research of optimal clamping pressure were reviewed and promising solutions for enhanced in-situ characterisation techniques were suggested. It is also important to mention that a part of the article was dedicated to electrochemical techniques that have been widely employed for in-situ investigations on the effects of mechanical stresses on PEMFC performance.

In order to assess the effects of assembly pressure on FC performance, several characterisation techniques have been used in the literature. Two main types of characterisations are currently employed: (1) - ex-situ, where the individual components are characterised externally to the FC, (2) - and in-situ, where the components are characterised within a FC operating in real-life conditions. Thus far, two familiar methods, in addition to continuous cell voltage monitoring, have been typically reported in the literature to study the effects of assembly pressure, namely polarisation curves and Electrochemical Impedance Spectroscopy (EIS) methods. Through employing these characterisation techniques (i.e. ex-situ and in-situ), a number of researchers working on the characterisation of PEMFCs are placing their focus on some particular issues: (1) - GDL electro-physical properties [30-32]; (2) - mass transport limitations [33-35]; (3) - durability [36-38]; (4) - water transport

visualisation techniques [39-41]; and (5) - pressure distribution [22-25]. Due to the complexity of the occurring phenomena, PEMFCs must be diagnosed using suitable techniques that allow both the evaluation of all the presented issues and the separation of their respective impacts on the overall FC performance.

Until now, numerous characterisation techniques have been reported in the literature to assess the FC performance. A number of reviews focusing on the characterisation techniques for PEMFCs have already been reported. Wu et al. [42] presented a review of the diagnostic tools employed in PEMFC using electrochemical techniques. Arvay et al. [43] reported a review of the characterisation techniques for GDLs used in PEMFCs. Their study focused on the essential properties of GDL, i.e. thermal and electrical conductivity, porosity, pore size, gas permeability, and wettability. The authors regrouped a set of tools used for the evaluation of GDLs by the use of in-situ and ex-situ characterisation techniques and concluded that the employment of both in-situ and ex-situ techniques is of significant importance towards developing high-performance GDLs.

Whilst a number of studies in the literature have focused on the ex-situ characterisation techniques to investigate the effect of mechanical compression on the FC performance [44-47], others employed both ex-situ and in-situ techniques with less focus on the latter [48-49]. Some review studies have also been reported in the literature so far [16,15,50]. In all these studies, it was well recognised that mechanical stress is one of the main factors that affect PEMFC performance. In a recent review on the effect of mechanical compression and dimensional change analysis on PEMFC components [7], a special attention has been attributed to the GDLs, and a range of dedicated characterisation methods have been presented (e.g. measurements of strain-stress curves for GDLs). In their manuscript, Millichamp et al. [15] provided a good state-of-the-art review regarding these issues, with an important focus on ex-situ characterisation techniques. A number of clamping methods

described in the academic and patent literatures has also been presented. However, no direct conclusion was drawn since there were no comparative studies on the different clamping procedures [15]. In another study, Dafalla and Jiang [16] reported a comprehensive review of the mechanical stresses and their related effects on structural properties of PEMFC components and performances. The authors reviewed different sources of stress within the cell and their respective impacts on its performance deterioration as well as the induced structural damage of the FC components. The report concluded that a comprehensive understanding of the combined realistic effects of mechanical stresses might be of major influence on the enhancement of FC performance.

In the characterisation works based on electrochemical techniques, some authors emphasised that higher clamping pressure gives best PEMFC performance whereas others reported that minimal clamping pressure, which ensures gas tight operation, needs to be considered for PEMFCs. However, most of the studies suggested optimal clamping pressure that gives a trade-off between the reduction in the ohmic resistance and the mass transport resistance after GDL deformation to be most desirable towards achieving high PEMFC performance. Nonetheless, the lack of cohesion in the reported studies (clamping methods, PEMFC components and design, operating conditions) makes it hardly possible to draw general conclusions regarding optimal clamping pressure. Typically, the average clamping force for PEMFCs can range from around 1 to 5 MPa, but more often around 1 to 2 MPa. As already mentioned, studies dealing with the research of optimal clamping pressure were already reviewed in [29], but the following are a few examples of in-situ experimental works available in the literature.

Ous and Arcoumanis [51] have used a FC compression unit to apply compressive loads on a single cell. Increasing the compression from 0 to 2 MPa improved the FC performance, with more considerable improvement in the ohmic region compared to the mass transport one.

However, as the compression exceeded 5 MPa, the FC performance declined drastically. This result was attributed to two main factors: the deflection of the plates in the compression unit leading to an increase in the internal resistance of the FC, and the decrease in the GDL porosity as the compression loads become more important.

Chang et al. [52] investigated a single cell with three GDL types. The assembly pressure was applied using a test fixture allowing the compression to be applied through a push rod driven by a pneumatic cylinder. For the three GDLs used, it was found that the peak power density reached its maximum at a compression of 3 MPa. The authors reported that higher compression loads (over 3 MPa) resulted in a decrease in FC performance. This finding was explained by some ex-situ measured changes in the GDL's electro-physical properties (gas permeability, water contact angle, and in-plane electrical resistivity) as the compression exceeded 3 MPa. Similar results were reported in [48,53,54] where a trade-off between the contact resistance and the mass transport resistance proved to give the best FC performance.

In [55], Irmscher et al. used a mechanical compression unit to determine the optimum clamping pressure for three commonly used GDLs. Compression levels were ranging from 0.1 to 2.7 MPa. The work shows that the optimum window for the mechanical pressure very much depends on the GDL type used and its properties (porosity, structure, and permeability).

Ahmad et al. have developed a spring equivalent PEMFC model which can predict the compression force required to obtain optimal performances [56,57]. In [57], in order to validate their model, Ahmad et al. have experimentally determined the optimal performance of a 4-cell stack. The change in stack voltage, resistance and maximum power was observed for different GDL compression levels. Peak power was measured at 1.55 MPa. The increase in resistance after this point was attributed to the mass transport losses at higher compression. Losses in the mass transport region were considered more important than gains made in the ohmic region as a result of increased compression.

Optimal clamping forces within the range of 1 to 2 MPa have also been suggested in various scientific studies and research papers dealing with modelling and simulation of certain PEMFC configurations [58-66]. While these papers discuss clamping forces and their effects on PEMFC performance, the specific values they suggest may also vary depending on modelling assumptions, on the data used for simulated materials, components and cell designs, as well as for virtual operating conditions.

Considering the complexity of the phenomena occurring within the PEMFC, combining in-situ and ex-situ characterisation techniques is of paramount importance in order to evaluate the effects of mechanical compression and deconvolute their specific impacts on the overall performance of the PEMFC. The objective of our work is, therefore, to investigate the effects of mechanical compression on the PEMFC performance through: i) the use of in-situ characterisation techniques and ii) the study of the correlations with the ex-situ results conducted within the framework of the research project (i.e. MIREPOIx project) that regroups both in-situ and ex-situ studies [29,44,67-70]. In this sense, this article aims to provide a thorough understanding of how mechanical compression quantitively affects PEMFC global performance. Investigations are conducted by combining cell voltage monitoring and polarisation curve measurements analysis (as well as EIS records; not presented in this article but available in [67]). These investigations are realised using different experimental procedures that represent, as closely as possible, the operating conditions of the FC during its lifelong operation. The analysis provided in this article gives insight into the enhancement of PEMFC performance through optimising the assembly pressure and provides guidelines for researchers and industrials to further understand the effects of mechanical compression in order to optimise the PEMFC performance.

The Graphical abstract illustrates the typical sandwich structure of a single-cell PEMFC with its components, namely the membrane (PEM), the Catalyst Layers (CLs), the Gas Diffusion

Layers (GDLs) with their Micro Porous Layers (MPLs), and the Flow Field Plates (FPPs) or BiPolar Plates (BPPs) at anode and cathode. The figure shows, in a stylised way, the impact of mechanical compression on the cell in terms of size change and electrical performance variation. Also, it indicates both the various characterisation means that are used in our research project to assess the PEMFC performance at global and local levels, and the focus in this article on cell voltage monitoring and polarisation curve recording. Investigations of the global cell response using EIS as well as analyses of the local phenomena in the cell under mechanical compression are suitable for future publications and information can already be found in [43].

This article proceeds as follows. We first outline in Section 2 the experimental setup developed and used in our work, namely the FC testbench, the specific mechanical compression unit and its instrumentation as well as a description of the constituent components of the PEMFC. We then present the experimental procedures employed in our experiments (Section 3). Following that, in the next two Sections (4 to 5), we analyse the results obtained and provide quantitative results regarding impacts of the mechanical compression on the phenomena occurring within the PEMFC. More precisely, Section 4 is dedicated to the study of the PEMF performance through cell voltage monitoring, Section 5 to the analysis based on polarisation curve measurements. Correlations with the results of the ex-situ GDL characterisation techniques are given throughout these last two Sections.

2. The experimental means

A specially designed test equipment was developed in order to experimentally investigate the effects of mechanical compression on the PEMFC performance. This apparatus allows combined electrical and mechanical characterisations of a single cell PEMFC subjected to various operation conditions and mechanical compression. This equipment includes:

- A PEMFC test bench: dedicated to the control and monitoring of the reactant gases, cell temperature, and the electric load. The FC bench can be connected to an Electrochemical Impedance Spectroscopy (EIS) station.
- A Mechanical Compression Unit (MCU): for the application of controlled mechanical compression to a PEMFC single cell assembly with an active area of 225 cm^2 (a large surface area, corresponding to those used in mobile or stationary applications).

Figure 1. depicts the main parts of the developed apparatus. In the following subsections, more details are given on each part of the equipment developed during this work as well as on the PEMFC investigated.

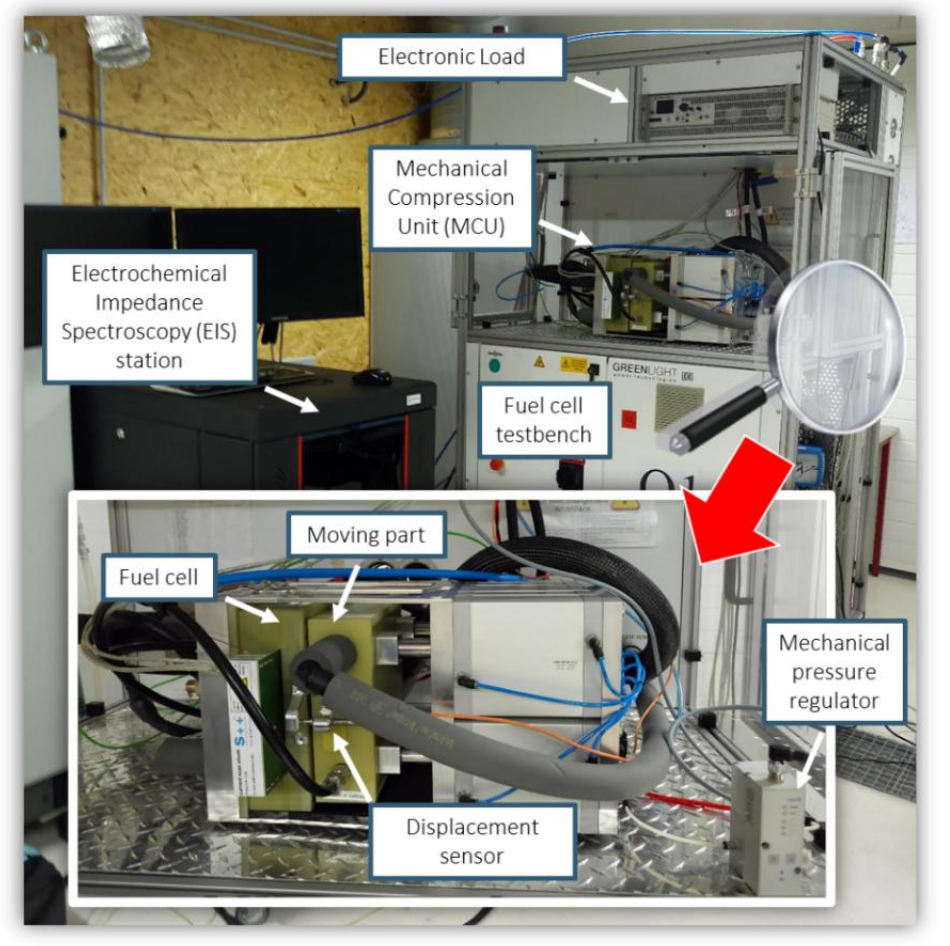

Fig. 1. Pictures of the experimental means developed and used in this study.

2.1. PEMFC test bench

The PEMFC test bench is a 1.5 kW test bench (G7805 from Greenlight Innovation® [71], Canada) allowing to reach a maximum current density of 2.2 A.cm^{-2} for the investigated FC. The test bench is connected to the hydrogen platform facilities (fluid arrivals and electrical connections) and to the MCU. This FC test bench allows all the measurements necessary for the monitoring and the control of the PEMFC (e.g. cell voltage, flow rates, pressures, temperatures). The test bench is controlled using a dedicated control and automation software developed by Greenlight Innovation® (i.e. HyWARE II™). The G7805 test bench is composed of three main parts. The first one includes the complete gas conditioning system, namely gas flows, temperatures and pressure controls, and gas humidification subsystem. The

second part includes the electronic management system and a DSLV1520 electronic load (Höcherl & Hackl [72], Germany) (as well as an EIS station [67]). Finally, the third part is made of the peripherals necessary for the temperature control of the PEMFC, namely the cooling / heating circuit and its equipment. A simplified block diagram of a FC test bench, quite similar to the one used in this study, has been published in [73]. A description of the fuel, oxidant, and temperature control circuits can be found in [67].

2.3. Mechanical Compression Unit (MCU)

A custom-built Mechanical Compression Unit (MCU), quickCONNECT fixture FC225 (batlticFuelCells [74], Germany), was specially designed for our test requirements. The MCU comes with four pneumatic cylinders that are capable of exerting a continuously adjustable mechanical compression (up to 2.15 MPa) on a single-cell PEMFC (active area of 225 cm²). The rapid fixing module (i.e. quickCONNECT fixture - qCf) allows precise assembly of the cell components (FFPs, GDLs, MEA) in a relatively straightforward and fast manner. Figure 2. depicts the MCU and its operating principle.

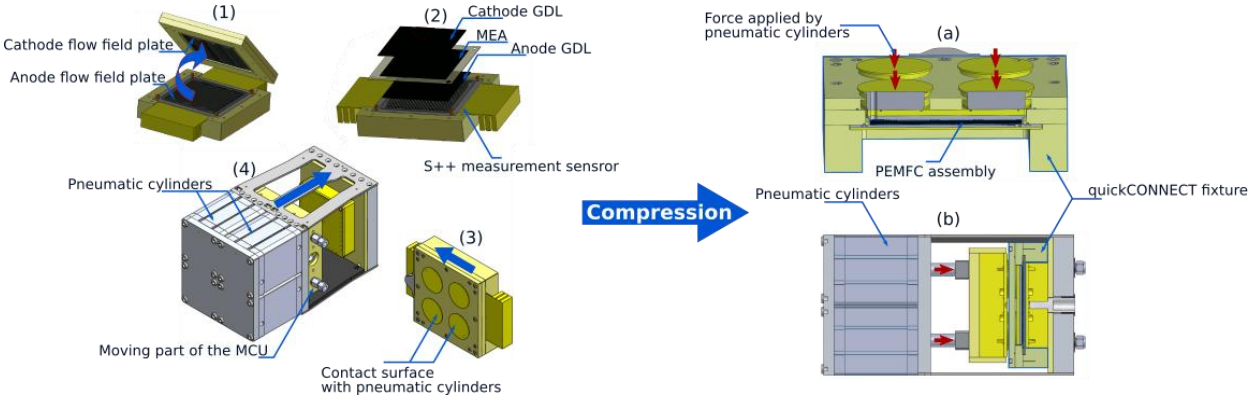

Fig. 2. Mechanical compression unit. Left: (1) opening of the qCf, (2) assembly of the PEMFC components, (3) placement of the qCf, (4) application of the mechanical assembly compression by the four pneumatic cylinders (images courtesy of balticFuelCells GmbH,

Germany). Right: Compression process of the MCU: (a) uncompressed qCf, (b) compressed qCf (images courtesy of balticFuelCells GmbH, Germany).

In order to get a thorough understanding of the effects of mechanical compression on PEMFC performance, the MCU was instrumented and equipped with: i) a proportional pressure regulator that allows the regulation of the mechanical compression with a dynamic resolution of 0.02 MPa; ii) a displacement sensor with a dynamic resolution of 1 µm (spring returned D6/01000A from RDP Group, UK [75,67]); and iii) a sensor for measuring the distributions of the current and the temperature (S++®, Germany [76,67]), with 441 and 49 current and temperature measuring points, respectively. This cell fixture was developed to allow accurate and repeatable characterisation of the FC components under different operating conditions and assembly pressure. More details about the mechanical compression regulation system are given below. Additional information about the other instrumentations (mechanical displacement measurement sensor, S++® device) can be found in [67].

The proportional pressure regulator (FESTO [77], Germany) is used to accurately control and measure the pressure inside the four pneumatic cylinders. The main characteristics of this device are as follows. The pressure regulation ranges from 0.1 to 10 bars. Nitrogen is used as an operating medium. The linearity error and the repetition accuracy are equal to 2 % and 0.5 % respectively (full scale).

The force per unit area (in $N.mm^{-2}$ or MPa) of the FC is calculated from the pressure inside the MCU pneumatic cylinders along with the backpressure inside the PEMFC components (i.e. reactive gas pressure in the channels of the FFPs) regulated at the anode and cathode compartments. These two pressures, one linked to the area of the pneumatic cylinders and the other to the surface of the FFPs channels, result in forces with opposite directions:

- The pressure of the gas (nitrogen) contained in the four pneumatic cylinders that apply a mechanical force on the FC assembly.

- The pressure of the reactants (H2 and air) contained in the FC (in the GDLs and FFPs). This pressure tends to separate the cell's components from one another.

The pressure exerted by the pneumatic cylinders must therefore counteract the pressure of the reactants present inside the cell. The two antagonistic pressures are linked to two opposing surfaces: the support surface of the cylinders on the one hand, and the surface of the channels in the FFPs on the other.

According to the manufacturer of the MCU (i.e. balticFuelCells), the mechanical force per unit area of the PEMFC can be calculated using Equation 1. In this Equation, the area of the pneumatic cylinders is equivalent to the surface of a cylinder with a radius "R = 125 mm", while the area of the flow field channels (under-channel regions) is equivalent to the surface of a cylinder with a radius "r = 70 mm". Therefore, the mechanical force per unit area of the PEMFC (P_{MPa}) can be calculated using Equation 1, which reflects a sum of forces:

$$P_{MPa} = \pi \frac{R^2 p_{cyl} - r^2 p_{bp}}{A} \times 10^{-1} \quad (1)$$

Where:

- P_{MPa} is the mechanical pressure (MPa or $N.mm^{-2}$) per unit area of the PEMFC.
- p_{cyl} is the pressure (bar) in the pneumatic cylinders, measured from the outlet of the proportional pressure regulator.
- p_{bp} is the backpressure (bar) of the PEMFC, measured from the backpressure regulators of the FC test bench (a backpressure of 0.5 barg was adopted to control the pressure of the FC reactants in our experimental investigations).

- A is the active area of the FC (22 500 mm^2).

2.4. The PEMFC components

The PEMFC investigated in this study was assembled using the quickCONNECT fixture. Information on the single cell components (MEA, GDLs, FFPs) are given below and in [67].

- Membrane Electrode Assembly (MEA): a three-layer MEA with a 225 cm^2 active area was used in this study. This MEA contains CLs with 0.2 and 0.4 mg $Pt.cm^{-2}$ at the anode and cathode sides, respectively. The membrane is a Nafion™ XL, which is based on a reinforced and chemically stabilised perfluoro sulfonic acid (PFSA) polytetrafluoroethylene (PTFE) copolymer. This reinforcement enhances the membrane physical properties [78,79]. The choice of the MEA is based on the enhanced performance of the Nafion™ XL membrane and also the Pt loading that is comparable to what is actually found real-life operating PEMFC used, for instance, in transportation applications [80].

- Gas Diffusion layer (GDL): the GDL used is a Sigracet® 38 BC (SGL Carbon [81], Germany), which is a non-woven carbon paper, MPL-coated, and PTFE-treated GDL. The Sigracet® 38 BC is considered as a low porosity GDL compared to other types (e.g. Sigracet® 39 BC [82]) and it is, therefore, more suited for operating conditions below 50%RH [82].

- Flow Field Plates (FFPs): graphite FFPs (grade FU 4369 HT) were used in our experimentation (from Schunk [83], Germany), both at anode and cathode sides. These FFPs consist of a parallel serpentine (12 parallel channels) design with channel and land width of 1 and 0.96 mm, respectively.

3. Experimental protocols and methods

In order to provide a thorough understanding of how mechanical compression quantitatively affects PEMFC performance, investigations are conducted by combining cell voltage monitoring and polarisation measurements analysis with the cell under mechanical constraints. These investigations are realised using different experimental procedures that represent, as closely as possible, the operating conditions of the FC during its lifetime operation.

Information on the experimental procedures and FC test conditions applied in our investigations are given below.

3.1. Leak tests and break-in procedures

Before going into the details of the experimental campaign conducted in this study, it seems important to mention that leak test and break-in procedures were applied prior the experimental campaign.

Leak tests were conducted in order to verify that the PEMFC and the test bench were gas-tight. They were performed following the harmonised test protocols for PEMFC testing in single-cell configuration for automotive applications proposed by the European FCs and Hydrogen Joint Undertaking (FCH-JU) [84]. Leak tests have enabled to define a minimum compression threshold (equal to 0.35 MPa) to be applied to ensure the tightness of the PEMFC.

Break-in procedures are typically applied to a newly assembled FC and have a lifelong effect on the PEMFC materials and performance, they are also likely to have a permanent bias of the test results when inappropriate break-in procedure is conducted during the early life of the FC [85]. In our study, two types of break-in procedures were applied, namely electrochemical and mechanical procedures, which are described hereafter.

- Electrochemical break-in procedure: this break-in procedure was conducted following a protocol adapted from the harmonised PEMFC testing for automotive applications, recommended by the European FCH-JU [84]. The recommended stability criterion that marks the end of the break-in procedure depends on the PEMFC voltage fluctuation and it is considered satisfied when it is lower than ±5 mV at the end of the break-in protocol. This criterion was accomplished in our break-in protocol (which lasted about 6 hours) since during the last 30 minutes the PEMFC voltage was fluctuating at less than ±5 mV.

- Mechanical break-in procedure: in order to exclude the effects of the first mechanical compression cycles on the PEMFC performance [47,69], a mechanical break-in protocol was conducted following an in-house developed procedure that consists of applying hundreds of compression cycles, ranging from 0.35 MPa to 2 MPa, prior to the experimental investigations described hereafter.

3.2. PEMFC operating and conditioning conditions

- Operating conditions: the PEMFC was maintained at constant temperature (60°C). It was operated under air / H_2 at fixed cathode and anode flowrates, which resulted in better stability of the cell voltage compared to fixed stoichiometry. This gas control mode was required to be able to observe the impacts of mechanical load changes (which led to small voltage variations as it will be addressed later on in this article). For the rest of this study, the PEMFC was operated at constant flowrates that were found optimal for a current density of 0.9 A cm^{-2} (air and H_2 flow rates equal to 19.1 and 2.4 $Nl.min^{-1}$). The reactants were supplied in flow-through mode at anode and cathode backpressures of 50 kPa. Hydrogen and air were used as reactants in co-flow mode, and this choice was motivated by a better current density distribution of the co-flow mode compared to counter-flow mode considering our operating conditions. The hydrogen was provided by a gas producer and distributor (Messer, France [86]) with a 5.0

quality (i.e. composition of H_2 > 99,999%). It has to be mentioned that several experimental investigations were conducted prior to the experimental design presented in this section: different levels of cell temperature, of gas flows, pressures and humidity rates were considered. The goal was to ascertain the optimal operating conditions for our PEMFC components. Then, the determined optimal operating conditions deduced from the aforementioned experimental investigations were held constant throughout the investigation presented in this article, and only the operating conditions allowing to investigate the effects of mechanical compression on the PEMFC performance were varied in this study (Section 3.3).

- PEMFC conditioning: the purpose of the PEMFC conditioning protocol is to ensure that the operating conditions we consider optimal for our study (i.e. cell temperature of 60°C, air and H_2 flow rates equal to 19.1 and 2.4 $Nl.min^{-1}$ respectively, anode and cathode backpressures of 50 kPa) are maintained constant and that the cell voltage is sufficiently stable before conducting our experimental investigations [67]. The conditioning protocol was considered as achieved when the voltage stability criterion, which is in our study defined based on the voltage fluctuation over the last 30 minutes, is lower than ± 5 mV. This conditioning protocol was systematically applied before each experimental investigation reported in this article. At the end of each experimentation, a shut-down protocol is conducted, which consists of inerting the PEMFC with nitrogen while reducing the cell temperature to ambient temperature under mechanical compression of 0.35 MPa.

3.3. Ranges of parameters studied

Real-life operating PEMFCs, especially in the transportation and portable applications, must provide stable performance over a wide range of operating conditions (e.g. pressure, temperature, shocks and vibrations). Given the fact that the operating conditions of the studied

PEMFC were kept constant, we have been particularly interested in this paper in the variation of three operating conditions, namely mechanical compression, current density, and reactants relative humidity (which is rarely done or reported in academic literature). Hence, twelve levels of mechanical compression, ranging from 0.35 MPa to 2 MPa with 0.15 MPa increments, were applied to the PEMFC. These mechanical compression levels were studied at current densities of 0.6 $A.cm^{-2}$ and 0.9 $A.cm^{-2}$, which are representative of regions where the ohmic and mass transport losses have relatively important values and will be referred to as medium and high current density, respectively. Finally, the tests were conducted under cathode and anode reactants humidification of 50%RH and 100%RH. In fact, the GDL provider (i.e. SGL Carbon) indicated that the Sigracet® 38 BC used in our study operates best at relative humidity less than or equal to 50%RH. As a part of the investigations intended to determine the optimal operating condition of the PEMFC components, we concluded that the optimal humidification of the reactants is 50%RH. Therefore, this value is used for the majority of the experimentations reported in this paper. However, a 100%RH was also used to further investigate the effect of water flooding on the PEMFC performance when subjected to mechanical compression. During all the experimentations, the relative humidity was changed simultaneously at the anode and cathode sides. Henceforth, whenever the relative humidification is mentioned, it concurrently refers to the cathode and anode sides.

3.4. Mechanical compression protocols

In this study, we have investigated two mechanical compression profiles as depicted in Fig. 3. The first, shown in Fig. 3 (a), represents a complete mechanical compression cycle, from 0.35 MPa to 2 MPa, and from 2 MPa back to 0.35 MPa, with steps of 0.15 MPa per 300 seconds. The duration of the mechanical compression levels was chosen to allow materials to be settled and performance to be stabilised before going from one mechanical compression to another.

The objective of using this profile (Fig. 3 (a)) is to finely investigate the effect of the increase and also the decrease of the mechanical stress inside the FC. From a real-life perspective, this mechanical compression protocol is representative of the mechanical stresses that can gradually be created and vanished inside the PEMFC (e.g. the mechanical stresses generated during the PEMFC assembly process, freeze/thaw cycles, and hygrothermal stresses generated as a result of the swelling/shrinking of the membrane). The second profile, depicted in Fig. 3 (b), is intended to reproduce randomised mechanical compression levels in order to minimise the effects of material memory, and therefore to reduce the impacts of gradual water accumulation with increasing mechanical compression [67]. In fact, as mechanical compression gradually increases, pores of GDLs get clogged and fibres of GDLs intrude into the FFPs channels leading to the worsening of the water management capability of the PEMFC. This latter effect leads to a progressive creation of water clusters within the PEMFC components.

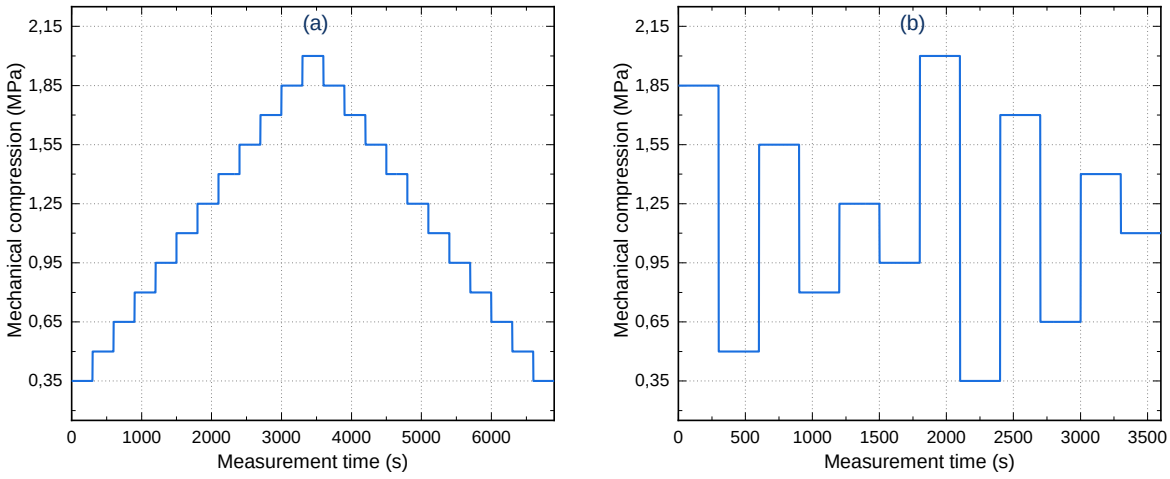

Fig. 3. Mechanical compression profiles. (a) gradual increase/decrease of mechanical compression; (b) randomised mechanical compression levels.

3.5. Combining electrochemical characterisations and mechanical compression protocols

Testing FCs through electrochemical characterisation techniques may take many forms. In our study, cell voltage monitoring and polarisation curve analysis were combined to investigate the FC performance using the mechanical compression profiles described in Fig. 3. The test procedures were defined by the combination of electrochemical characterisation methods and mechanical compression protocols as follows:

- Cell voltage monitoring (Section 4) with two mechanical compression profiles: gradual increase / decrease, and randomised.
- Polarisation curve measurements (Section 5) with randomised mechanical compression profile.

Before conducting each of these characterisation techniques, a first conditioning cycle was systematically applied as detailed in Section 3.2.

The analyses of the next Sections 4 and 5 are intended to provide guidelines for researchers and industrials to further understand the effects of mechanical compression in order to optimise the PEMFC performance. The results obtained will be analysed and quantitative results concerning the impacts of mechanical compression on the phenomena occurring in the PEMFC will be provided. Correlations with ex-situ results will be given throughout the Sections 4 and 5.

4. Cell voltage monitoring

The FC voltage was measured for every level of mechanical compression as depicted in Fig. 3 (a) and (b). The use of two different mechanical compression profiles is intended to represent, as closely as possible, the mechanical stresses underwent by FCs during their lifetime operations. The voltage monitoring was conducted for two current density values, namely 0.6

A.cm^{-2} and 0.9 A.cm^{-2}, and under two levels of anode and cathode relative humidity of 50%RH and 100%RH. The results obtained at the highest current density level (i.e. 0.9 A.cm^{-2}) will be presented in more detail in this article.

4.1. Gradual increase/decrease of mechanical compression (results at 0.9 A.cm^{-2})

The voltage measurements as a function of mechanical compression are shown in Fig. 4. for a current density of 0.9 A. cm^{-2}. The voltage was measured at cathode and anode relative humidity of 50%RH and 100%RH. Some 150 voltage measurements per mechanical compression cycle were plotted and a second-order polynomial curve fitting was used to analyse the trend of the voltage evolution as a function of mechanical compression. The coefficients of determination (i.e. R-squared value) of the fitted curves were higher than 0.9.

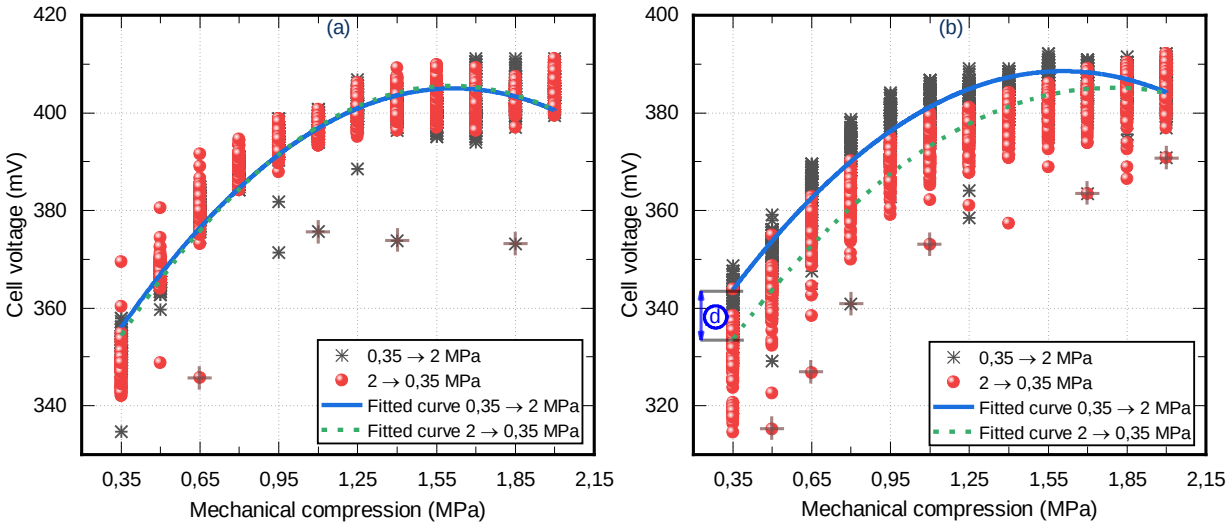

Fig. 4. Voltage monitoring as a function of mechanical compression at 0.9 A.cm^{-2}. (a) 50%RH and (b) 100%RH. Region (d) shown in Fig. 4. (b) shows the voltage difference after one mechanical compression cycle and (+) symbols depict examples of voltage drops due to water accumulation/reactants starvation.

The measured cell voltage at 50%RH is higher than the one at 100%RH at 0.9 A.cm^{-2} (similar results are obtained for current density 0.6 A.cm^{-2} [67]), with a voltage difference value of 14 mV. This voltage difference can be attributed to the liquid water accumulation caused by operating the PEMFC at a high relative humidity of 100%RH. This effect led to the formation of water clusters that clog the GDLs pores and the FFPs channels leading to an increase in the mass transport losses of the PEMFC.

With regards to the voltage evolution with mechanical compression, it can be seen that it increases first with increasing mechanical compression up to 1.55 MPa then it reaches a plateau or even starts to decrease. At 0.9 A.cm^{-2}, the increase in the cell voltage from 0.35 MPa to 1.55 MPa is measured to be +48.8 mV and +44.7 mV at 50%RH and 100%RH, respectively (at 0.6 A.cm^{-2}: +18.8 mV and +18 mV, respectively [67]). A decreasing voltage tendency starting from 1.7 MPa up to 2 MPa can be seen in Fig. 4. In order to confirm the decrease of cell voltage after 1.7 MPa, further investigation needs to be carried out at compression levels above 2 MPa. However, this was not feasible in our study as increasing the mechanical compression beyond this level was not attainable using our apparatus. Nevertheless, this would not be practically recommended in real-life operating PEMFCs [29].

As indicated in the introduction to the article and in [29], the optimum compression to be applied to the PEMFC is usually between 1 and 2 MPa, which is in good agreement with our results. In the literature, the exact optimal pressure can vary based on the type of materials used, on the specific cell and stack design, and the manufacturer's recommendations. Factors that influence the optimal clamping force include: - Component materials, structures, surface properties, and thicknesses; - Clamping solutions, designs of the cells and stacks; - Operating conditions: cell temperature, gas pressure, flow and humidity rates within the FC.

The results obtained by Ahmad et al. [56,57] and mentioned in their work (a plateau of voltage was demonstrated between 1.55 and 1.65 MPa of GDL compression, with a maximum

power at 1.55 MPa) look very similar to ours, perhaps due to the characteristics of the components used (similar GDL thickness of 325 μm) and the operating conditions, which could be quite similar.

Related results concerning the optimum level of compression have also been obtained in modelling/simulation by various research teams. For example, using a numerical study, Xiaohui Yan et al. [62] found that the power of a stack can be maximised for pressures ranging from 1.5 to 3.5 MPa owing to the balanced mass transport and contact resistance. A compression of 1.5 MPa even enables the lowest voltage difference (5.4 mV) among the individual cells in the stack studied, which is beneficial for the cell-to-cell consistency. A finite element model was developed by Carral and Mélé to study the mechanical state of PEMFC stacks with a variable number of cells [64,65]. The average contact pressure between the FFP and the (MEA+GDLs) set is found almost constant and independent of cell number, ranging from 1.4 to 1.6 MPa, close to values found by Bates et al. [66] in a comparable study. This is also close to the compression recommended by the US Department of Energy for GDL / FFP interfacial contact resistance measurements (1.4 MPa) [80].

Thus, increasing the PEMFC assembly pressure beyond 2 MPa could lead to a notable increase in the mass transport resistance and also to irreversible damage of the PEMFC components (including GDL materials and structure) [87-89] and will not be, therefore, addressed in this study. Regarding cell voltage variations, it can be observed from Fig. 4. that the cell voltage is less stable at 100%RH compared to 50%RH. This observation is related to the water accumulation leading to voltage drops as depicted by (+) signs in Fig. 4. (b). These voltage drops are more frequent during the backward mechanical compression sweep compared to the forward one. It can also be seen from Fig. 4. (b) that the PEMFC presented lower voltage during the backward sweep of mechanical compression. The region depicted by (d) in Fig. 4. (b) shows voltage difference after one cycle of mechanical compression. This

voltage difference is also present in Fig. 4. (a) and it is caused by the gradual accumulation of water after increasing the mechanical compression up to 2 MPa. This effect is more discernible (around 10 mV difference) at 0.9 $A.cm^{-2}$ and 100%RH where more water is produced and introduced though fully humidified reactants to the PEMFC.

During this experimental procedure, it was shown that the cell voltage was higher in the forward mechanical compression sweep compared to the backward one. This effect is more pronounced at the end of the mechanical compression cycle (see region (d) in Fig. 4. (b)). Since all the operating conditions that contribute to the formation of liquid water were held constant all along the experimentation, this water cluster formation is therefore attributed solely to the effect of increasing mechanical compression, which leads to the GDLs pores blockage and fibres intrusion into the flow fields channels, leading to a formation of water clusters that increase the gas diffusion losses and therefore reduce the cell voltage after one cycle of mechanical compression. Although the technique of increasing (and less commonly increasing/decreasing) mechanical load was largely employed in the literature [29,15,16], this technique may not be fully representative of the stresses endured by PEMFC during their lifetime operation. Therefore, in order to reduce the effects of water accumulation due to the gradual increase of mechanical compression, the following subsection employs the same voltage monitoring technique while using a randomised mechanical compression profile as show in Fig. 3. (b).

4.2. Randomised mechanical compression profile

In this second experimental procedure, randomised mechanical compression levels were applied to the FC as depicted in Fig. 3. (b). As mentioned earlier in this article, employing this mechanical compression profile eliminates the effect of gradual water accumulation. Figure 5. shows the results from voltage measurement at 0.6 $A.cm^{-2}$ and 0.9 $A.cm^{-2}$ using randomised

mechanical compression protocol. These voltage measurements were conducted for both 50%RH and 100%RH.

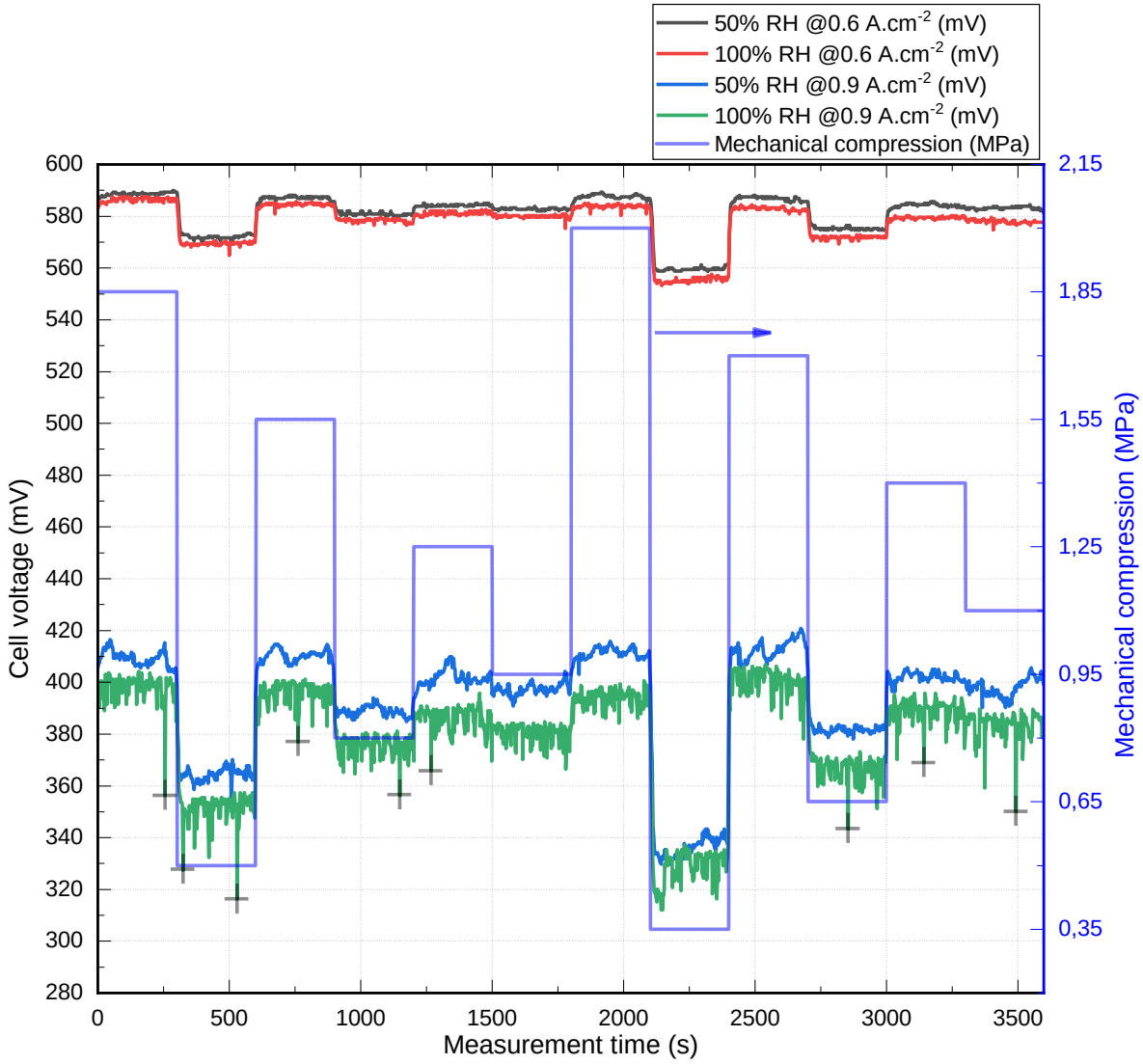

Fig. 5. Voltage evolution using randomised mechanical compression protocol. (+) signs indicate examples of voltage drops due to liquid water accumulation/reactants starvation. The voltage curves are presented in the same order as the ones in the figure's label (top to bottom).

It can be observed from Fig. 5. that the mechanical compression affects the PEMFC voltage at all tested current density and relative humidity ranges. Also, the voltage loss due to the increase in the relative humidity is more important at high current density, where the average

voltage difference between tests at 50%RH and 100%RH is measured to be 3.55 mV and 11.22 mV at 0.6 A.cm^{-2} and 0.9 A.cm^{-2} respectively. Figure 5. also shows that the FC voltage at 100%RH is substantially unstable compared to 50%RH, which is mainly due to water clusters formation leading to reactants starvation and therefore voltage drops (as depicted by the (+) signs in Fig. 5). These voltage drops are more recurrent at the 0.9 A.cm^{-2} and 100%RH where more water is brought to the FC through the humidifiers and also where more water is generated at the cathode side as a product of the cell reaction on the CL. Also, and in line with the results reported using the first experimental procedure, it can be observed from Fig. 5. that mechanical compression affects, with a more pronounced manner, the cell voltage when the PEMFC is operating at 0.9 A.cm^{-2} compared to 0.6 A.cm^{-2}. This effect is explained by the important effects of reducing the ohmic losses at high current density compared to medium current density due to better membrane hydration state [67] this effect will be addressed in more detail later in this article. Data from Fig. 5. are reported in Fig. 6. with average and standard deviation values per each level of mechanical compression. Figure 6. shows that the mechanical compression improves the PEMFC voltage at all tested operating conditions, with a major voltage improvement at a mechanical compression up to 1.55 MPa.

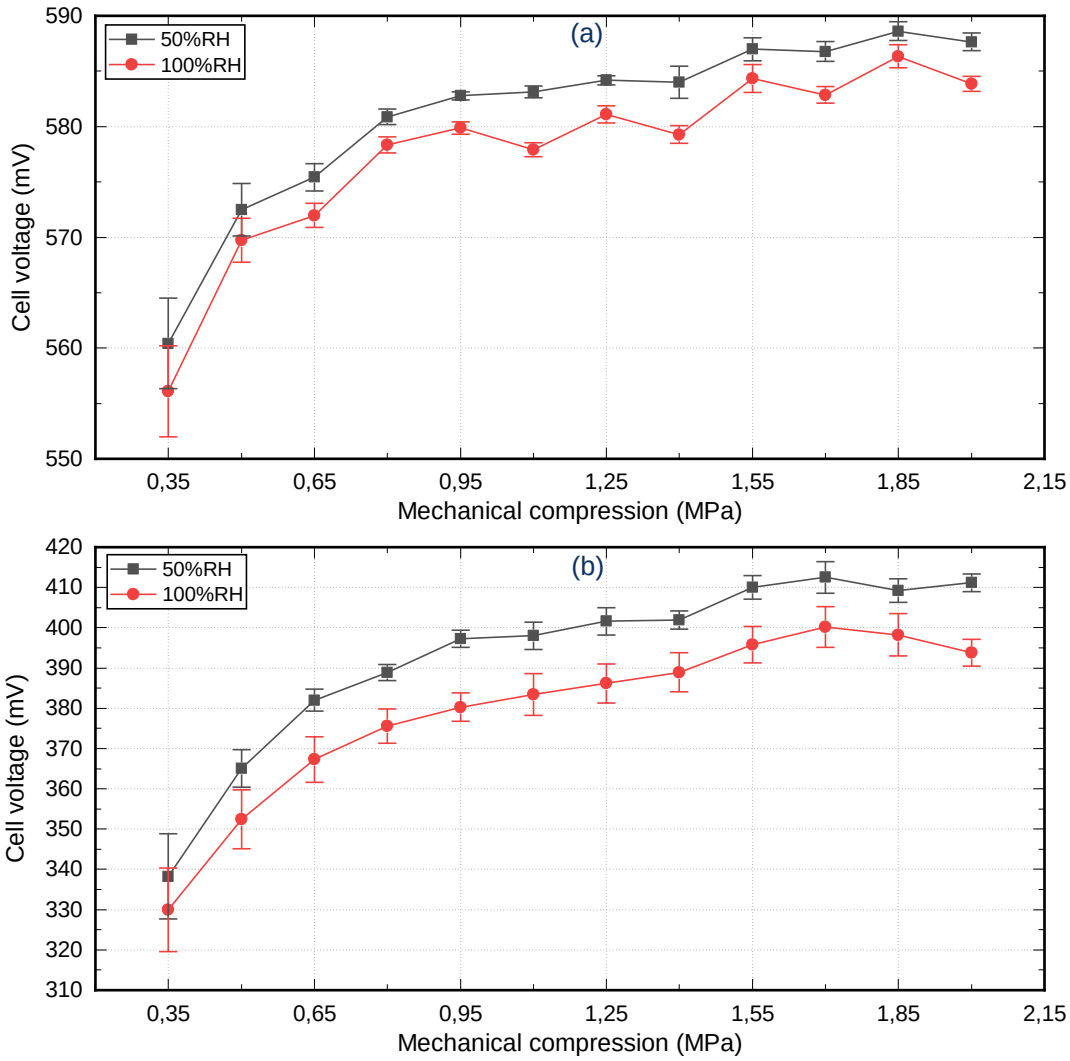

Fig. 6. Voltage evolution using randomised mechanical compression protocol at 50%RH and 100%RH. (a) at 0.6 A.cm^{-2} and (b) at 0.9 A.cm^{-2}.

The average voltage improvement from 0.35 MPa to 1.55 MPa at both 50%RH and 100%RH is measured to be +27.5 mV and +68.8 mV at 0.6 A.cm^{-2} and 0.9 A.cm^{-2}, respectively. This difference in voltage increase as a function of mechanical compression is attributed to the higher effect of reducing the ohmic resistance at higher current densities (0.9 A.cm^{-2}) compared to medium current densities (0.6 A.cm^{-2}). This effect can be explained by the fact that since our PEMFC was operated at fixed flowrates corresponding to a current density of 0.9 A.cm^{-2}, the membrane endures liquid water evacuation due to the relatively high flowrates

at 0.6 A.cm^{-2}, and therefore increasing the protonic resistance of the membrane. These results are in good agreement with the finding of Felix Buchi et al. [90]. These authors measured the ohmic resistance at 60°C of a FC design with forced reactants flowrates to be 11.4% higher than in a design without forced flowrates. This effect seems to be more dominant in our study, as the voltage increase as a function of mechanical compression is 13% higher at 0.9 A.cm^{-2} compared to 0.6 A.cm^{-2}. This effect may be explained by the fact that when the FC is compressed, GDL pores get clogged, which increases the water concentration gradient at the cathode side, leading to a more pronounced back diffusion mechanism of water. Therefore, more water is kept inside the membrane, which in turn improves the voltage of the PEMFC through reducing the protonic resistance of the membrane. These results are also in good agreement with the finding of Cha et al. [91]. These authors carried out a study on the effects of assembly pressure on PEMFC performance. They reported that the ohmic resistance decreased with increasing the assembly pressure. This result was attributed not only to the decrease in the electronic contact and bulk resistances of the PEMFC components but also to the increase in the membrane hydration. This latter was associated with the reduction in the GDL porosity with increasing the assembly pressure leading to a substantial back-diffusion water transport mechanism from the cathode to the anode side, which induces better membrane hydration state and leads to the reduction in the membrane protonic resistance. This effect will be addressed in more detail later in this article.

During these first two experimental procedures, i.e. FC voltage monitoring using i) gradual increase/decrease and ii) randomised mechanical compression protocols, the PEMFC was operated at a fixed electronic load value. These experimental procedures are representative of the effects of mechanical compression on PEMFC operating at a fixed electronic load point. The goal of the following section is to investigate the effects of mechanical compression on a FC operating in a dynamic electronic load condition.

5. Polarisation curve measurements

5.1. Results

The polarisation curve analysis is one of the most common techniques used for global PEMFC performance assessment. This technique involves an increasing and/or decreasing sweep of electrical load in order to obtain a characteristic of the PEMFC voltage as a function of current density (i.e. galvanostatic mode) for specified operating conditions. In our study, the current was controlled using a ramp load profile under specified operating conditions as reported in Section 3.2. The electronic load was varied following a smooth ramp sweep with 2.2 $mA.cm^{-2}$ per second (7 minutes on average per each polarisation curve measurement). The mechanical compression was applied following the randomised mechanical compression profile as presented in Fig. 3. (b). The polarisation curve measurements were conducted at both 50%RH and 100%RH anode and cathode relative humidity. Figure 7. shows the polarisation curves of 12 levels of randomised mechanical compression at anode and cathode relative humidity of 50%RH and 100%RH.

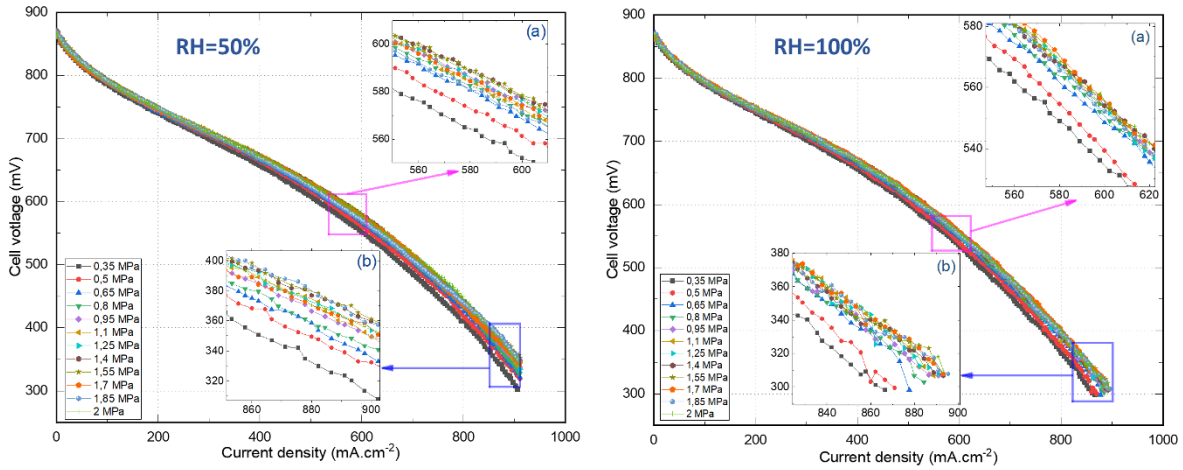

Fig. 7. Polarisation curves for 12 randomised levels of mechanical compression at 50%RH (left) and 100%RH (right). Inserts (a) and (b) are zoomed-in regions representative of the ohmic and mass transport losses, respectively.

Results from Fig. 7. show the impact of mechanical compression on PEMFC performance. The zoomed-in inserts (a) and (b) correspond to regions where the ohmic and mass transport losses have relatively important values, respectively. It can be observed that the PEMFC voltage increases with increasing mechanical compression at all current density ranges, with a substantial increase from 0.35 to 0.95 MPa. For better readability, the results from Fig. 7. corresponding to 0.6 and 0.9 A.cm^{-2} are reported in Fig. 8.

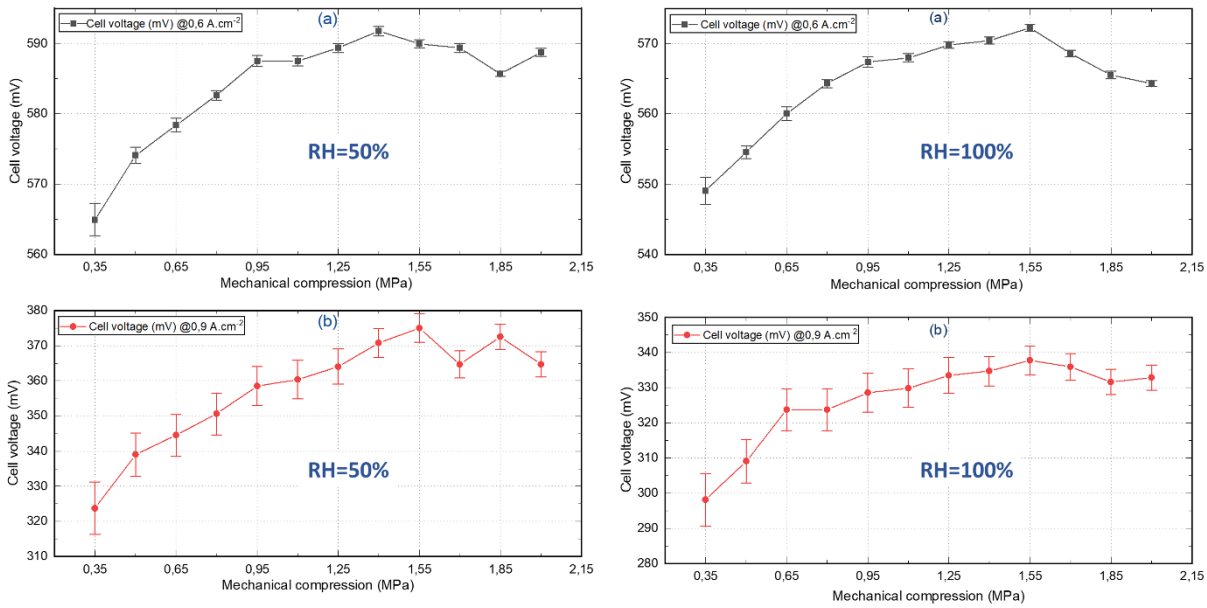

Fig. 8. Voltage evolution as a function of mechanical compression: (a) at 0.6 A.cm^{-2} and (b) at 0.9 A.cm^{-2}, at 50%RH (left) and 100%RH (right). The data are obtained from Fig. 7.

Figure 8. (left, (a) and (b)), related to the results obtained at 50%RH, shows that as the mechanical compression increased from 0.35 MPa to 1.55 MPa, the cell voltage was

improved by 4.3% (+25.1 mV) and 13.7% (+51.3 mV) at current densities of 0.6 A.cm^{-2} and 0.9 A.cm^{-2}, respectively. Therefore, the voltage improvement with mechanical compression at high current density is more pronounced (9.4 % higher) compared to medium current density, which is in good agreement with the results reported using the first two experimental procedures. These results are attributed to the better membrane humidification at high current density compared to medium one. Detailed explanations are given at the end of this subsection.

The same experimental procedure used for tests at 50%RH was conducted at 100%RH. The results (Fig. 7. (right) and Fig. 8. (right, (a) and (b))) show comparable voltage evolution trends, with a lower overall performance at 100%RH (+23.3 mV at 0.6 A.cm^{-2} and +39.7 mV at 0.9 A.cm^{-2}) compared to 50%RH.

5.2. Comparison of steady-state experimental procedures results

In this Section, we compare the different test results obtained using the steady-state electrochemical characterisation techniques (i.e. cell voltage monitoring and polarisation curve measurements) and the associated mechanical compression profiles (i.e. as depicted in Section 3.5).

5.2.1. Effect of mechanical compression on cell voltage stability

With regards to voltage stability, results from the first experimental procedure (i.e. cell voltage monitoring) show that mechanical compression reduces the voltage standard deviation at both 50%RH and 100%RH. Figure 9. shows the cell voltage standard deviation evolution as a function of mechanical compression at 0.6 A.cm^{-2}. The voltage standard deviation was calculated from 300 measurement points combining forward and backward mechanical compression sweeps.

Although the effect shown in Fig. 9. is complex to describe, two plausible causes may be evoked here. The first is related to the ohmic resistance of the GDL. In fact, since the GDL used in our study was subjected to hundreds of mechanical compression cycles, the GDL fibres might be crushed [89], and some small GDL fibres fragments may get to slightly move with reactants and water flows at mechanical compression below 0.8 MPa. The movements of these GDL fibres fragments modifies the ohmic resistance through changing the electrical contact positions of the GDL fibres and, therefore, contributing to the cell voltage instability. As the mechanical compression reaches 0.8 MPa (Fig. 9.), the GDL material and fibres are settled and the cell voltage reaches its maximum stabilisation level.

The second possible cause of the results presented in Fig. 9. may be attributed to the PEMFC water management when it is subjected to mechanical stresses, and some related explanations can be found in the literature. Indeed, some studies reported correlations between the water management related issues and the mechanical stresses applied to the PEMFC. One of the main subjects of debate is the preferential pathways for liquid water transport within the GDL when subjected to mechanical compression. In fact, some authors reported that water is preferentially transported in the compressed regions beneath the ribs [92-94] whereas others reported the areas beneath the channels as preferential pathways for water transport [95,96]. Since mechanical compression was shown to improve the FC voltage stability, it seems that in our case the liquid water is preferentially located in the regions beneath the ribs, where water accumulation is less critical compared to the regions beneath the channels at where water clusters may cause reactants starvation and therefore voltage instability. With this regard, Bazylak et al. [92] investigated the effect of mechanical compression on liquid water transport within the GDL. These authors reported that liquid water is located in the regions beneath the ribs. This finding was attributed to PTFE coating and carbon fibres damage, which led to hydrophobic content degradation in the compressed regions of the GDL. This effect favours

water accumulation in the compressed GDL regions (FFPs ribs) compared to the uncompressed ones (FFPs channels). The same effect was reported in an in-situ study by Forner-Cuenca et al. [97]. This water accumulation might be beneficial for FC voltage stability since water is located beneath the ribs where its accumulation is less critical than regions beneath the channels where reactants are supplied to the reaction sites.

In line with Bazylak et al. [92], Ince et al. [93] investigated the in-plane water transport in both the compressed and the uncompressed regions of the GDLs. These authors emphasised that mechanical compression improves the in-plane water transport in the compressed regions of the GDL. Hartnig et al. [94] employed synchrotron X-ray radiography to visualise water locations in an operating PEMFC and reported that water agglomerates mainly beneath the ribs of the FFPs. The experimental findings of [92-94] are in good agreement with the results presented in Fig. 9. Since mechanical compression promotes water agglomeration in the regions beneath the FFPs' ribs and improves the in-plane transport of liquid water in the compressed GDL regions. Therefore, these phenomena reduce the voltage fluctuation due to water clusters formation beneath the channels and, as a result, improve the voltage stability.

The results reported in Fig. 9. Are only related to a current density of 0.6 $A.cm^{-2}$. The voltage stability evolution at 0.9 $A.cm^{-2}$ has not suggested any discernible trend as a function of mechanical compression. This is attributed mainly to the higher presence of liquid water at the cathode side at 0.9 $A.cm^{-2}$ due to its generation as a result of the cathode reactions, which gives fairly unstable cell voltage independently from the mechanical compression (Fig. 8.). It has to be noted that only possible causes of the effect are presented in Fig. 9. Are given in this section. However, future studies need to be carried out in order to conduct in-situ investigations on the water clusters location as a function of mechanical compression as this subject was not comprehensively discussed in the literature [29]. Moreover, other phenomena may contribute to the stabilisation of the cell voltage with increasing mechanical compression

(e.g. improvement in the electrical and thermal conductivities of the PEMFC components, reduction in the leak rate of reactants) and could be the subject of future research activities.

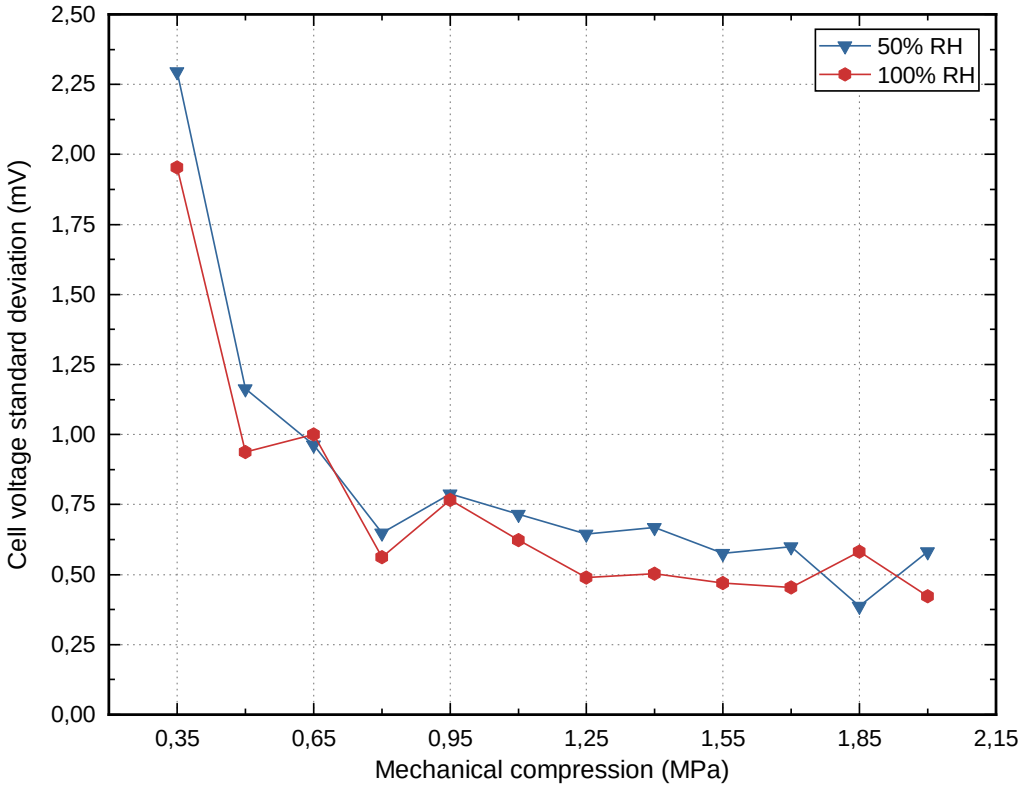

Fig. 9. Cell voltage standard deviation as a function of mechanical compression at 0.6 A.cm^{-2}.

5.2.2. Effect of mechanical compression on cell voltage evolution

Figure 10. shows the average voltage evolution measured using the three experimental procedures reported in this section. The mechanical compression is divided into two ranges: from 0.35 MPa to 1.55 MPa (blue bars) and from 1.55 to 2 MPa (orange bars), hereafter referred to as the first and second compression range, respectively. The goal of gathering the results from all three experimental procedures is to investigate the effect of mechanical compression on the PEMFC performance independently from the experimental procedure used.

It can be observed from Fig. 10. that mechanical compression improves the PEMFC voltage during the first compression range (i.e. from 0.35 MPa to 1.55 MPa) at all tested operating conditions. This effect of voltage improvement is preeminent at high current density (0.9 A.cm^{-2}) compared to medium current density (0.6 A.cm^{-2}) at all operating conditions range. The voltage evolution shows a decreasing tendency starting from 1.55 MPa to 2 MPa. The explanations of these effects will be addressed in more detail in the following subsections.

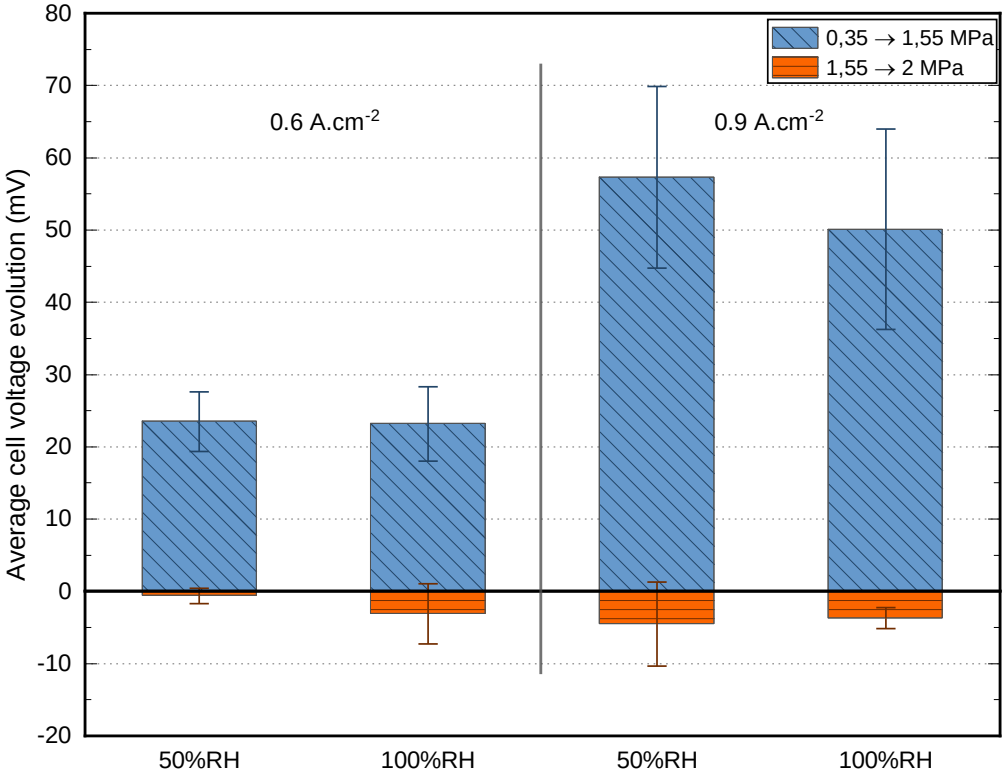

Fig. 10. Cell voltage evolution over the compression range 0.35 → 2 MPa using the cell voltage monitoring and polarisation curve measurements.

- **At medium current density:** the FC voltage evolution at 0.6 A.cm^{-2} over the first and second compression ranges is shown in Fig. 10. It can be observed that the cell voltage increases during the first compression range. This voltage increase is attributed to the dominance of the reduction in the ohmic resistance against the increase in the mass transport

losses. Similar results are observed at both 50%RH and 100%RH at the first compression range and are attributed to the fact that the PEMFC was operated at fixed flowrates adapted for 0.9 $A.cm^{-2}$. These flowrates are high enough to allow the evacuation of the produced water at 0.6 $A.cm^{-2}$. Therefore, no substantial mass transport losses were taking place at this compression range. However, as the compression exceeded 1.55 MPa, the cell voltage was further decreased at 100%RH compared to 50%RH. This effect is mainly due to the excess water brought to the PEMFC through the fully humidified gases at 100%RH. This effect, added to the fact that the PEMFC was further compressed up to 2 MPa, led to a decrease in the GDL porosity that, in turn, induced higher mass transport losses at 100%RH.

As mentioned before, the voltage increase during the first mechanical compression range is caused mainly by the decrease in the ohmic resistance of the PEMFC components. This ohmic resistance comprises the protonic resistance of the membrane and the electronic resistance of the PEMFC components [98]. This latter includes the bulk resistance of the FC components and the contact resistance at the interfaces between the MEA, MPL, GDL, and the FFPs [47]. The ohmic resistance is generally attributed to the protonic resistance of the membrane. However, when it comes to mechanical stresses related issues, the electronic resistance, and more importantly the electronic contact resistance, contributes substantially to the total ohmic resistance of the PEMFC. This effect was previously reported in the literature, Nitta et al. [99], for instance, reported that uneven assembly pressure may increase the contact resistance, and it may even attain the same order of magnitude as the membrane resistance. This finding is more important to emphasise as the pressure inhomogeneity is a common issue in real-life operating PEMFCs assembled using point-load design using typical fastener of bolts and nuts [18,24,51,100].

With this regard, the improvement of the cell voltage during the first compression range at 0.6 $A.cm^{-2}$, as shown in Fig. 10., is attributed up to a certain extent to the reduction in the

electronic resistance of the PEMFC components. One of the main contributions to this electronic resistance comes from the interfacial contact resistance. Indeed, in a study carried out within the framework of our research project (i.e. MIREPOix project), K. Bouziane et al. conducted an ex-situ investigation on the effects of cyclic mechanical compression (Fig. 11.) on the electrical contact resistance between the GDLs and the adjacent PEMFC components using a number of commercially available GDLs [68,69]. In this study, and for in-situ/ex-situ comparison purposes, we have decided to present solely the results of the Sigracet® 24 BC GDL, which has the most similar characteristics (compared to other GDLs used in the ex-situ study) with the Sigracet® 38 BC used in our in-situ investigations, and which is provided by the same company (SGL carbon [101]). The main characteristics of the Sigracet® 24 BC GDL (straight carbon fibre paper with MPL coating) are as follows [102]: PTFE load of 5%, porosity of 40%, area weight of 100 g m^{-2}, thickness of 235 µm, and through-plane gas permeability of 5.09 × 10^{-12} m^2. It can be observed from Fig. 11. that the mechanical compression reduces the electrical contact resistance, with a 68% reduction attained at 1.5 MPa over a 71% reduction at 2 MPa. These results show that the major reduction of the contact resistance occurs at 1.5 MPa, which is in good agreement with our in-situ results shown in Fig. 10. The diminution in the contact resistance shown in Fig. 11. (b) is attributed to the improvement in the electrical contact between the GDL and the adjacent components and to the reduction in the GDLs porosity, which increases carbon fibre electrical connections leading to a reduced electrical resistivity between the GDLs fibres [69]. This effect, which was also reported in an ex-situ study carried out by Qiu et al. [103], seems to be dominant over the increase in the gas diffusion losses in our in-situ study. Therefore, these combined reductions in the bulk and contact resistances noticeably led to the increase in the FC voltage during the first compression range as shown in Fig. 10.

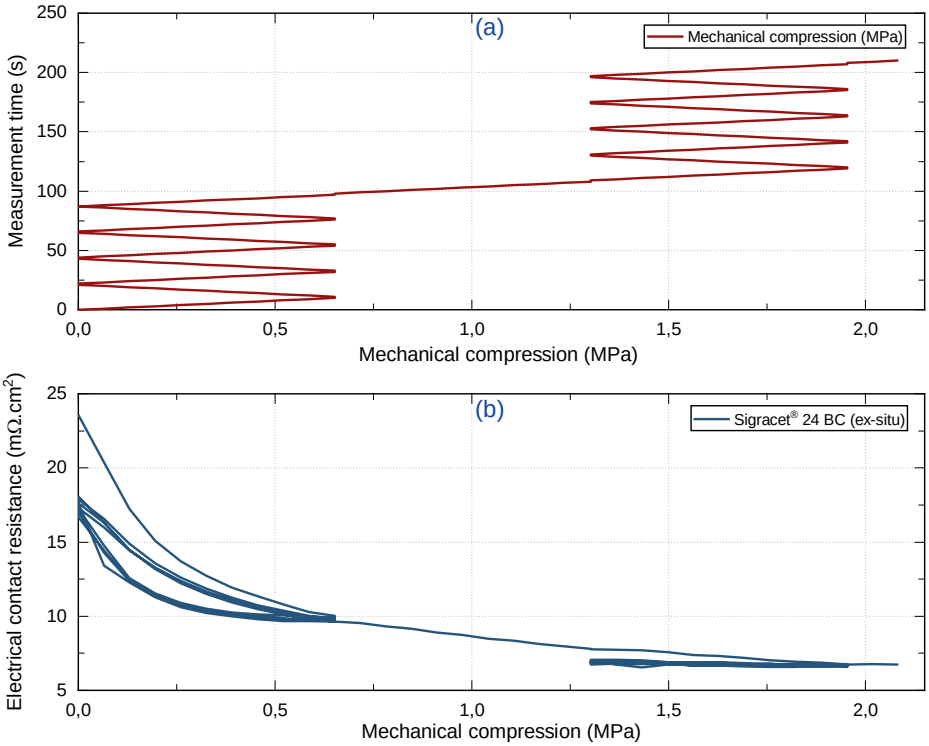

Fig. 11. Effect of mechanical compression on the contact resistance (a) Mechanical compression profile used in the ex-situ study (b) The electrical contact resistance of the GDL as a function of mechanical compression.

- At high current density: it can be observed from Fig. 10. that the FC voltage was improved with increasing mechanical compression at the first compression range. This effect is attributed to the dominance of the decrease in the ohmic resistance against the increase in the mass transport losses for a compression up to 1.55 MPa. This voltage improvement was measured to be 14.4% higher at 50%RH compared to 100%RH. This voltage improvement difference is explained by the high mass transport losses that occur when the reactant gases are fully humidified at 100%RH. During the second compression range (i.e. from 1.55 MPa to 2 MPa), the voltage decreased at the same order of magnitude, which is mainly due to the increase in the gas diffusion losses as a result of the decrease in the GDLs' porosity with increasing mechanical compression beyond 1.55 MPa.

Figure 10. also emphasises an outstanding comparison concerning the voltage improvement at the first compression range, which is ~twice as much higher at 0.9 A.cm^{-2} compared to 0.6 A.cm^{-2}. Considering the operating conditions of the PEMFC used in this study, the higher voltage increase at high current density is mainly attributed to the reduction of the protonic resistance of the membrane with increasing mechanical compression. In fact, at 0.9 A.cm^{-2}, more water is formed at the cathode side (compared to 0.6 A.cm^{-2}) as a product of the electrochemical reactions on the CL. Moreover, the GDLs porosity decreases with higher mechanical compression and, therefore, liquid water is kept at the cathode CL side. This water agglomeration creates a concentration gradient that induces the transport of a part of the accumulated water from the cathode to the anode side (i.e. back diffusion process [104,105]) through the membrane, which improves and homogenises the hydration state of the membrane and, in turn, reduces its protonic conductivity as illustrated in Fig. 12. These results are in good agreements with the finding of Cha et al. [91], these authors reported that the ohmic resistance of the PEMFC decreased with increasing the current density, which was attributed to the better membrane hydration at high current densities due to the increase in water production rate at the cathode side.

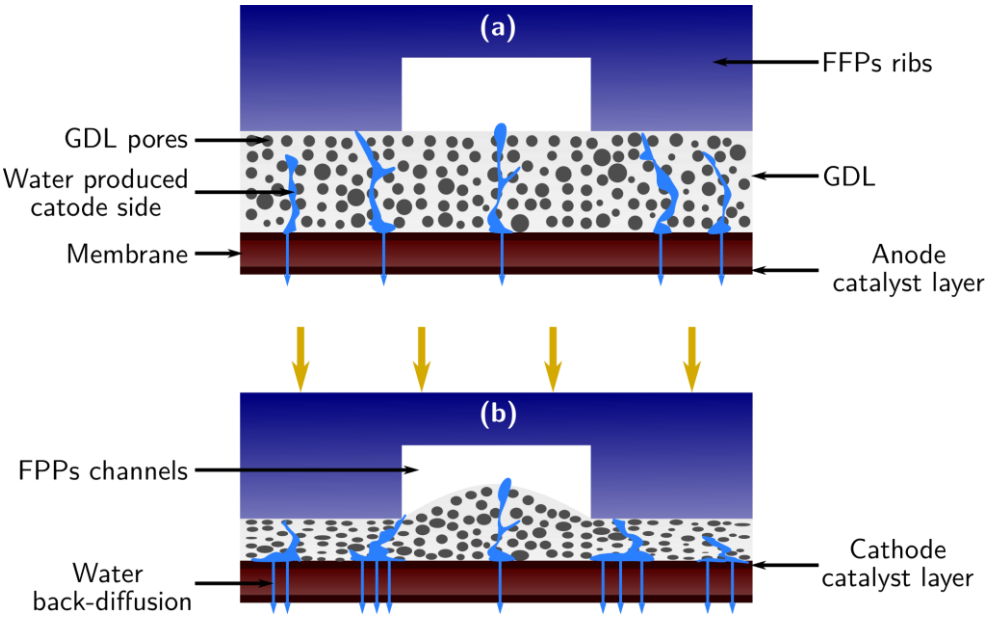

Fig. 12. Effect of mechanical compression on the back-diffusion process of water (blue arrows). (a) uncompressed GDL and (b) compressed GDL.

7. Conclusion

This article provides a thorough study of the effects of mechanical compression on the global performance of a PEMFC. The investigations were carried out using polarisation curve analysis and FC voltage monitoring, and correlated with ex-situ characterisations (contact resistances between FFP and GDL). In this study, 12 levels of mechanical compression were investigated, ranging from 0.35 MPa to 2 MPa with steps of 0.15 MPa. These investigations were carried out in two different ways: using gradual increase / decrease of mechanical loads as well as randomised mechanical compression protocols. Results of steady-state characterisation techniques showed that mechanical compression (i.e. up to 1.55 MPa) improves the PEMFC performance at all tested operating conditions. This finding was attributed to the dominant reduction of the ohmic resistance against the increase of mass transport losses. It was also shown that a mechanical compression level higher than 1.55 MPa does not result in any further improvement of the FC voltage, it may even worsen the PEMFC performance due to the increase in the reactant transport losses. Therefore, the presented results suggest that compressing the PEMFC beyond a specified level (i.e. 1.55 MPa) would not lead to any further improvement of the PEMFC performance. This level of compression is in line with ex-situ characterisations of GDL contact resistances carried out in our laboratory [68,69], and also appears to be consistent with various experimental and simulation findings from other research teams [29,56,57,62,64-66,80].

In order to better understand these results, further studies are being carried out as part of this research project. They include analyses of EIS as well as mechanical pressure and temperature distributions in the cell. The results of these studies are to be published.

Acknowledgments

The “Région Bourgogne-Franche-Comté” is gratefully acknowledged for its support through the ELICOP Project (Ref. 2015C-4944 and 2015-4948) and the co-funding of KHETABI El Mahdi’s PhD thesis (Convention N° 2017 Y_07529). The authors would also like to gratefully acknowledge 3M and Plastic Omnium for the support given to this research project.

References

[1] Larminie J, Dicks A. Introduction. Fuel Cell Systems Explained, John Wiley & Sons, Ltd; 2013, p. 1-24. https://doi.org/10.1002/9781118878330.ch1.

[2] Capurso T, Stefanizzi M, Torresi M, Camporeale SM. Perspective of the role of hydrogen in the 21st century energy transition. Energy Conversion and Management 2022;251:114898. https://doi.org/10.1016/j.enconman.2021.114898.

[3] Radhakrishnan V, Haridoss P. Effect of cyclic compression on structure and properties of a Gas Diffusion Layer used in PEM fuel cells. International Journal of Hydrogen Energy 2010;35(20):11107-11118. https://doi.org/10.1016/j.ijhydene.2010.07.009.

[4] García-Salaberri PA, Vera M, Zaera R. Nonlinear orthotropic model of the inhomogeneous assembly compression of PEM fuel cell gas diffusion layers. International Journal of Hydrogen Energy 2011;36(18):11856-11870. https://doi.org/10.1016/j.ijhydene.2011.05.152.

[5] Gigos PA, Faydi Y, Meyer Y. Mechanical characterization and analytical modeling of gas diffusion layers under cyclic compression. International Journal of Hydrogen Energy 2015;40(17):5958-5965. https://doi.org/10.1016/j.ijhydene.2015.02.136.

[6] Carral C, Mélé P. A constitutive law to predict the compression of gas diffusion layers. International Journal of Hydrogen Energy 2018; 43(42): 19721-19729. https://doi.org/10.1016/j.ijhydene.2018.08.210.

[7] Amit C. Bhosale, Raghunathan Rengaswamy. Interfacial contact resistance in polymer electrolyte membrane fuel cells: Recent developments and challenges. Renewable and Sustainable Energy Reviews 2019; 115:109351. https://doi.org/10.1016/j.rser.2019.109351.

[8] Keller N, Hübner P, Von Unwerth T. Investigation of intrusion effects of a gas diffusion layer into channel cross sections depending on channel parameters of metallic bipolar plates. International Journal of Hydrogen Energy 2020;45(30):15366-15379. https://doi.org/10.1016/j.ijhydene.2020.03.245.

[9] Uzundurukan A, Bilgili M, Devrim Y. Examination of compression effects on PEMFC performance by numerical and experimental analyses. International Journal of Hydrogen Energy 2020;45(60):35085-35096. https://doi.org/10.1016/j.ijhydene.2020.04.275.

[10] Afrasiab H, Davoodi KH, Barzegari MM, Gholami M, Hassani A. A novel constitutive stress-strain law for compressive deformation of the gas diffusion layer. International Journal of Hydrogen Energy 2022;47(75):32167-32180. https://doi.org/10.1016/j.ijhydene.2022.07.127.

[11] Jian Zhao, Xianguo Li. A review of polymer electrolyte membrane fuel cell durability for vehicular applications: Degradation modes and experimental techniques. Energy Conversion and Management 2019;199:112022. https://doi.org/10.1016/j.enconman.2019.112022.

[12] Novalin T, Eriksson B, Proch S, Bexell U, Moffatt C, Westlinder J, Lagergren C, Lindbergh G, Wreland Lindström R. Concepts for preventing metal dissolution from stainless-steel bipolar plates in PEM fuel cells. Energy Conversion and Management 2022;253:115153. https://doi.org/10.1016/j.enconman.2021.115153.

[13] Peng Liang, Diankai Qiu, Linfa Peng, Peiyun Yi, Xinmin Lai, Jun Ni. Contact resistance prediction of proton exchange membrane fuel cell considering fabrication characteristics of metallic bipolar plates. Energy Conversion and Management 2018;169:334-344. https://doi.org/10.1016/j.enconman.2018.05.069.

[14] Mahmoudi AH, Ramiar A, Esmaili Q. Effect of inhomogeneous compression of gas diffusion layer on the performance of PEMFC with interdigitated flow field. Energy Conversion and Management 2016;110:78-89. https://doi.org/10.1016/j.enconman.2015.12.012.

[15] Millichamp J, Mason TJ, Neville TP, Rajalakshmi N, Jervis R, Shearing PR, Brett DJL. Mechanisms and effects of mechanical compression and dimensional change in polymer electrolyte fuel cells - A review. Journal of Power Sources 2015;284:305-20. https://doi.org/10.1016/j.jpowsour.2015.02.111.

[16] Dafalla AM, Jiang F. Stresses and their impacts on proton exchange membrane fuel cells: A review. International Journal of Hydrogen Energy 2018;43:2327-48. https://doi.org/10.1016/j.ijhydene.2017.12.033.

[17] Zhou Y, Lin G, Shih AJ, Hu SJ. Multiphysics Modeling of Assembly Pressure Effects on Proton Exchange Membrane Fuel Cell Performance. J Fuel Cell Sci Technol 2009;6:041005-041005-7. https://doi.org/10.1115/1.3081426.

[18] Lee S-J, Hsu C-D, Huang C-H. Analyses of the fuel cell stack assembly pressure. Journal of Power Sources 2005;145:353-61. https://doi.org/10.1016/j.jpowsour.2005.02.057.

[19] Alizadeh E, Barzegari MM, Momenifar M, Ghadimi M, Saadat SHM. Investigation of contact pressure distribution over the active area of PEM fuel cell stack. International Journal of Hydrogen Energy 2016;41(4):3062-3071. https://doi.org/10.1016/j.ijhydene.2015.12.057.

[20] Alizadeh E, Ghadimi M, Barzegari MM, Momenifar M, Saadat SHM. Development of contact pressure distribution of PEM fuel cell's MEA using novel clamping mechanism. Energy 2017;131:92-97. https://doi.org/10.1016/j.energy.2017.05.036

[21] Montanini R, Squadrito G, Giacoppo G. Experimental evaluation of the clamping pressure distribution in a PEM fuel cell using matrix-based piezoresistive thin-film. Sensors 2009:6.

[22] Gatto I, Urbani F, Giacoppo G, Barbera O, Passalacqua E. Influence of the bolt torque on PEFC performance with different gasket materials. International Journal of Hydrogen Energy 2011;36:13043-50. https://doi.org/10.1016/j.ijhydene.2011.07.066.

[23] De la Cruz J, Cano U, Romero T. Simulation and in situ measurement of stress distribution in a polymer electrolyte membrane fuel cell stack. Journal of Power Sources 2016;329:273-80. https://doi.org/10.1016/j.jpowsour.2016.08.073.

[24] Wen C-Y, Lin Y-S, Lu C-H. Experimental study of clamping effects on the performances of a single proton exchange membrane fuel cell and a 10-cell stack. Journal of Power Sources 2009;192:475-85. https://doi.org/10.1016/j.jpowsour.2009.03.058.

[25] Barzegari MM, Ghadimi M, Momenifar M. Investigation of contact pressure distribution on gas diffusion layer of fuel cell with pneumatic endplate. Applied Energy 2020;263:114663. https://doi.org/10.1016/j.apenergy.2020.114663.

[26] C.W. Wu, W. Zhang, X. Han, Y.X. Zhang, G.J. Ma. A systematic review for structure optimization and clamping load design of large proton exchange membrane fuel cell stack. Journal of Power Sources 2020;476:228724. https://doi.org/10.1016/j.jpowsour.2020.228724.

[27] Diankai Qiu, Linfa Peng, Peiyun Yi, Werner Lehnert, Xinmin Lai. Review on proton exchange membrane fuel cell stack assembly: Quality evaluation, assembly method, contact behavior and process design. Renewable and Sustainable Energy Reviews 2021;152:111660. https://doi.org/10.1016/j.rser.2021.111660.

[28] Ke Song at al. Assembly techniques for proton exchange membrane fuel cell stack: A literature review. Renewable and Sustainable Energy Reviews 2022;153:111777. https://doi.org/10.1016/j.rser.2021.111777.

[29] Khetabi EM, Bouziane K, Zamel N, François X, Meyer Y, Candusso D. Effects of mechanical compression on the performance of polymer electrolyte fuel cells and analysis through in-situ characterisation techniques - A review. Journal of Power Sources 2019;424:8-26. https://doi.org/10.1016/j.jpowsour.2019.03.071.

[30] Chun JH, Park KT, Jo DH, Kim SG, Kim SH. Numerical modeling and experimental study of the influence of GDL properties on performance in a PEMFC. International Journal of Hydrogen Energy 2011;36:1837-45. https://doi.org/10.1016/j.ijhydene.2010.01.036.

[31] Ismail MS, Damjanovic T, Ingham DB, Pourkashanian M, Westwood A. Effect of polytetrafluoroethylene-treatment and microporous layer-coating on the electrical conductivity of gas diffusion layers used in proton exchange membrane fuel cells. Journal of Power Sources 2010;195:2700-8. https://doi.org/10.1016/j.jpowsour.2009.11.069.

[32] Lim C, Wang CY. Effects of hydrophobic polymer content in GDL on power performance of a PEM fuel cell. Electrochimica Acta 2004;49:4149-56. https://doi.org/10.1016/j.electacta.2004.04.009.

[33] Kong CS, Kim D-Y, Lee H-K, Shul Y-G, Lee T-H. Influence of pore-size distribution of diffusion layer on mass-transport problems of proton exchange membrane fuel cells. Journal of Power Sources 2002;108:185-91. https://doi.org/10.1016/S0378-7753(02)00028-9.

[34] Bultel Y, Wiezell K, Jaouen F, Ozil P, Lindbergh G. Investigation of mass transport in gas diffusion layer at the air cathode of a PEMFC. Electrochimica Acta 2005;51:474-88. https://doi.org/10.1016/j.electacta.2005.05.007.

[35] Park S, Popov BN. Effect of cathode GDL characteristics on mass transport in PEM fuel cells. Fuel 2009;88:2068-73. https://doi.org/10.1016/j.fuel.2009.06.020.

[36] Liu D, Case S. Durability study of proton exchange membrane fuel cells under dynamic testing conditions with cyclic current profile. Journal of Power Sources 2006;162:521-31. https://doi.org/10.1016/j.jpowsour.2006.07.007.

[37] Zhang S, Yuan X, Wang H, Mérida W, Zhu H, Shen J, Wu S, Zhang J . A review of accelerated stress tests of MEA durability in PEM fuel cells. International Journal of Hydrogen Energy 2009;34:388-404. https://doi.org/10.1016/j.ijhydene.2008.10.012.

[38] Wahdame B, Candusso D, Harel F, François X, Péra M-C, Hissel D, Kauffmann J-M. Analysis of a PEMFC durability test under low humidity conditions and stack behaviour modelling using experimental design techniques. Journal of Power Sources 2008;182:429-40. https://doi.org/10.1016/j.jpowsour.2007.12.122.

[39] Tüber K, Pócza D, Hebling C. Visualization of water buildup in the cathode of a transparent PEM fuel cell. Journal of Power Sources 2003;124:403-14. https://doi.org/10.1016/S0378-7753(03)00797-3.

[40] Satija R, Jacobson DL, Arif M, Werner SA. In situ neutron imaging technique for evaluation of water management systems in operating PEM fuel cells. Journal of Power Sources 2004;129:238-45. https://doi.org/10.1016/j.jpowsour.2003.11.068.

[41] Spernjak D, Prasad AK, Advani SG. Experimental investigation of liquid water formation and transport in a transparent single-serpentine PEM fuel cell. Journal of Power Sources 2007;170:334-44. https://doi.org/10.1016/j.jpowsour.2007.04.020.

[42] Wu J, Yuan XZ, Wang H, Blanco M, Martin JJ, Zhang J. Diagnostic tools in PEM fuel cell research: Part I Electrochemical techniques. International Journal of Hydrogen Energy 2008;33:1735-46. https://doi.org/10.1016/j.ijhydene.2008.01.013.

[43] Arvay A, Yli-Rantala E, Liu C-H, Peng X-H, Koski P, Cindrella L, et al. Characterization techniques for gas diffusion layers for proton exchange membrane fuel cells - A review. Journal of Power Sources 2012;213:317-37. https://doi.org/10.1016/j.jpowsour.2012.04.026.

[44] El Oualid S, Lachat R, Candusso D, Meyer Y. Characterization process to measure the electrical contact resistance of Gas Diffusion Layers under mechanical static compressive loads. International Journal of Hydrogen Energy 2017;42:23920-31. https://doi.org/10.1016/j.ijhydene.2017.03.130.

[45] Sadeghifar H, Djilali N, Bahrami M. Thermal conductivity of a graphite bipolar plate (BPP) and its thermal contact resistance with fuel cell gas diffusion layers: Effect of compression, PTFE, micro porous layer (MPL), BPP out-of-flatness and cyclic load. Journal of Power Sources 2015;273:96-104. https://doi.org/10.1016/j.jpowsour.2014.09.062.

[46] Prass S, Hasanpour S, Sow PK, Phillion AB, Mérida W. Microscale X-ray tomographic investigation of the interfacial morphology between the catalyst and micro porous layers in proton exchange membrane fuel cells. Journal of Power Sources 2016;319:82-9. https://doi.org/10.1016/j.jpowsour.2016.04.031.

[47] Sadeghifar H. In-plane and through-plane electrical conductivities and contact resistances of a Mercedes-Benz catalyst-coated membrane, gas diffusion and micro-porous layers and a Ballard graphite bipolar plate: Impact of humidity, compressive load and polytetrafluoroethylene. Energy Conversion and Management 2017;154:191-202. https://doi.org/10.1016/j.enconman.2017.10.060.

[48] Chang WR, Hwang JJ, Weng FB, Chan SH. Effect of clamping pressure on the performance of a PEM fuel cell. Journal of Power Sources 2007;166:149-54. https://doi.org/10.1016/j.jpowsour.2007.01.015.

[49] Lin J-H, Chen W-H, Su Y-J, Ko T-H. Effect of gas diffusion layer compression on the performance in a proton exchange membrane fuel cell. Fuel 2008;87:2420-4. https://doi.org/10.1016/j.fuel.2008.03.001.

[50] Zhang W, Wu C. Effect of Clamping Load on the Performance of Proton Exchange Membrane Fuel Cell Stack and Its Optimization Design: A Review of Modeling and Experimental Research. J Fuel Cell Sci Technol 2013;11:020801-020801-11. https://doi.org/10.1115/1.4026070.

[51] Ous T, Arcoumanis C. Effect of compressive force on the performance of a proton exchange membrane fuel cell. Proceedings of the Institution of Mechanical Engineers, Part C: Journal of Mechanical Engineering Science 2007;221:1067-74. https://doi.org/10.1243/09544062JMES654.

[52] Chang HM, Chang MH. Effects of Assembly Pressure on the Gas Diffusion Layer and Performance of a PEM Fuel Cell. Applied Mechanics and Materials 2012;110-116:48-52. https://doi.org/10.4028/www.scientific.net/AMM.110-116.48.

[53] Lee W, Ho CH, Van Zee JW, Murthy M. The effects of compression and gas diffusion layers on the performance of a PEM fuel cell. Journal of Power Sources 1999;84:45-51. https://doi.org/10.1016/S0378-7753(99)00298-0.

[54] Hassan NU, Kilic M, Okumus E, Tunaboylu B, Soydan AM. Experimental determination of optimal clamping torque for AB-PEM fuel cell. Journal of Electrochemical Science and Engineering 2016;6:9-16. https://doi.org/10.5599/jese.198.

[55] Irmscher P, Qui D, Janßen H, Lehnert W, Stolten D. Impact of gas diffusion layer mechanics on PEM fuel cell performance. International Journal of Hydrogen Energy 2019;44(41):23406-23415. https://doi.org/10.1016/j.ijhydene.2019.07.047.

[56] Ahmad M, Harrison R, Meredith J, Bindel A, Todd B. Analysis of the compression characteristics of a PEM stack, development of an equivalent spring model and recommendations for compression process improvements. IREC2015 The Sixth International Renewable Energy Congress, Sousse, Tunisia, 2015, pp. 1-6, doi: 10.1109/IREC.2015.7110935.

[57] Ahmad M, Harrison R, Meredith J, Bindel A, Todd B. Validation of a fuel cell compression spring equivalent model using polarisation data. International Journal of Hydrogen Energy 2017;42(12):8109-8118. https://doi.org/10.1016/j.ijhydene.2017.01.216.

[58] Xing XQ, Lum KW, Poh HJ, Wu YL. Optimization of assembly clamping pressure on performance of proton-exchange membrane fuel cells. Journal of Power Sources 2010;195(1):62-68. https://doi.org/10.1016/j.jpowsour.2009.06.107.

[59] Jiaran Liu, Jinzhu Tan, Weizhan Yang, Yang Li, Chao Wang. Better electrochemical performance of PEMFC under a novel pneumatic clamping mechanism. Energy 2021;229:120796. https://doi.org/10.1016/j.energy.2021.120796.

[60] Keller N, Von Unwerth T. Advanced parametric model for analysis of the influence of channel cross section dimensions and clamping pressure on current density distribution in PEMFC. Applied Energy 2022;307:118132. https://doi.org/10.1016/j.apenergy.2021.118132.

[61] Ouaidat G, Cherouat A, Kouta R, Chamoret D. Study of the effect of mechanical uncertainties parameters on performance of PEMFC by coupling a 3D numerical multiphysics model and design of experiment. International Journal of Hydrogen Energy 2022;47(56):23772-23786. https://doi.org/10.1016/j.ijhydene.2022.05.151.

[62] Le Carre T, Blachot JF, Poirot-Crouvezier JP, Laurencin J. Mechanical response of carbon paper gas diffusion layer under patterned compression. International Journal of Hydrogen Energy 2023. Available online 29 August 2023. https://doi.org/10.1016/j.ijhydene.2023.08.104.

[63] Xiaohui Yan, Chen Lin, Zhifeng Zheng, Junren Chen, Guanghua Wei, Junliang Zhang. Effect of clamping pressure on liquid-cooled PEMFC stack performance considering inhomogeneous gas diffusion layer compression. Applied Energy 2020;258:114073. https://doi.org/10.1016/j.apenergy.2019.114073.

[64] Carral C, Mélé P. A numerical analysis of PEMFC stack assembly through a 3D finite element model. International Journal of Hydrogen Energy 2014;39:4516-4530. https://doi.org/10.1016/j.ijhydene.2014.01.036.

[65] Carral C, Charvin N, Trouvé H, Mélé P. An experimental analysis of PEMFC stack assembly using strain gage sensors. International Journal of Hydrogen Energy 2014;39(9):4493-4501. https://doi.org/10.1016/j.ijhydene.2014.01.033.

[66] Bates A, Mukherjee S, Hwang S, Lee SC, Kwon O, Choi GH, Park S. Simulation and experimental analysis of the clamping pressure distribution in a PEM fuel cell stack. International Journal of Hydrogen Energy 2013;38 (15):6481-6493. https://doi.org/10.1016/j.ijhydene.2013.03.049.

[67] Khetabi EM. Behavioural analysis of PEM fuel cell components and research of causal relationships between in-situ and ex-situ observed performances. PhD Thesis of Université Paris-Saclay, 2021. https://theses.hal.science/tel-04055314.

[68] Bouziane K. Study of the relationship between the performance of PEM fuel cell components and their behaviours in stacks operated in the complete system. Development of electrical and mechanical characterization techniques. PhD Thesis of Université Paris-Saclay, 2021.

[69] Bouziane K, Khetabi EM, Lachat R, Zamel N, Meyer Y, Candusso D. Impact of cyclic mechanical compression on the electrical contact resistance between the gas diffusion layer and the bipolar plate of a polymer electrolyte membrane fuel cell. Renewable Energy 2020;153:349-61. https://doi.org/10.1016/j.renene.2020.02.033.

[70] Charbonné C, Dhuitte ML, Bouziane K, Chamoret D, Candusso D, Meyer Y. Design of experiments on the effects of linear and hyperelastic constitutive models and geometric parameters on polymer electrolyte fuel cell mechanical and electrical behaviour. International Journal of Hydrogen Energy 2021;46(26):13775-13790. https://doi.org/10.1016/j.ijhydene.2021.02.122

[71] Fuel Cell and Battery Test Equipment | Greenlight Innovation. https://www.greenlightinnovation.com/.

[72] The electronic load - Höcherl & Hackl. Höcherl & Hackl En. https://www.hoecherl-hackl.com/.

[73] Bégot S, Harel F, Candusso D, François X, Péra M-C, Yde-Andersen S. Fuel cell climatic tests designed for new configured aircraft application. Energy Conversion and Management 2010;51:1522-1535. https://doi-org.ezproxy.utbm.fr/10.1016/j.enconman.2010.02.011.

[74] balticFuelCells GmbH: Innovation in fuel cell technologies. https://www.balticfuelcells.de/defaultE.html.

[75] D5 & D6 LVDT Displacement Transducer. https://www.rdpe.com/ex/d5-d6.htm.

[76] S++ Simulation Services. http://www.splusplus.com/measurement/en/csshunt.html.

[77] FESTO. https://www.festo.com/net/en-gb_gb/SupportPortal/Default.aspx?q=554044.

[78] NafionTM XL. https://www.fuelcellstore.com/nafion-xl.

[79] Robert M, El Kaddouri A, Perrin J-C, Mozet K, Daoudi M, Dillet J, et al. Effects of conjoint mechanical and chemical stress on perfluorosulfonic-acid membranes for fuel cells. Journal of Power Sources 2020;476:228662. https://doi.org/10.1016/j.jpowsour.2020.228662.

[80] DOE Technical Targets for Polymer Electrolyte Membrane Fuel Cell Components. EnergyGov. https://www.energy.gov/eere/fuelcells/doe-technical-targets-polymer-electrolyte-membrane-fuel-cell-components.

[81] Fuel Cells on the Rise. SGL Carbon. https://www.sglcarbon.com/en/for-a-smarter-world/fuel-cells-on-the-rise/.

[82] (PDF) SIGRACET® Gas Diffusion Layers for PEM Fuel Cells, Electrolyzers and Batteries (White Paper). https://www.researchgate.net/publication/295859224_SIGRACETR_Gas_Diffusion_Layers_for_PEM_Fuel_Cells_Electrolyzers_and_Batteries_White_Paper.

[83] Bi-polar Plates. https://www.schunk-carbontechnology.com/en/products/produkte-detail/bipolar-plates.

[84] EU harmonised test protocols for PEMFC MEA testing in single cell configuration for automotive applications | EU Science Hub. https://ec.europa.eu/jrc/en/publication/eur-scientific-and-technical-research-reports/eu-harmonised-test-protocols-pemfc-mea-testing-single-cell-configuration-automotive.

[85] Bezmalinović D, Radošević J, Barbir F. Initial conditioning of Polymer Electrolyte Membrane fuel cell by temperature and potential cycling. Acta Chimica Slovenica 2014;62:83-7. https://doi.org/10.17344/acsi.2014.730.

[86] Gaz spéciaux - Messer France SAS. https://www.messer.fr/gaz-purs-et-melanges.

[87] Mason TJ, Millichamp J, Shearing PR, Brett DJL. A study of the effect of compression on the performance of polymer electrolyte fuel cells using electrochemical

impedance spectroscopy and dimensional change analysis. International Journal of Hydrogen Energy 2013;38:7414-22. https://doi.org/10.1016/j.ijhydene.2013.04.021.

[88] Kandlikar SG, Lu Z, Lin TY, Cooke D, Daino M. Uneven gas diffusion layer intrusion in gas channel arrays of proton exchange membrane fuel cell and its effects on flow distribution. Journal of Power Sources 2009;194:328-37. https://doi.org/10.1016/j.jpowsour.2009.05.019.

[89] Mason TJ, Millichamp J, Neville TP, El-kharouf A, Pollet BG, Brett DJL. Effect of clamping pressure on ohmic resistance and compression of gas diffusion layers for polymer electrolyte fuel cells. Journal of Power Sources 2012;219:52-9. https://doi.org/10.1016/j.jpowsour.2012.07.021.

[90] Büchi FN, Scherer GG. In-situ resistance measurements of Nafion® 117 membranes in polymer electrolyte fuel cells. Journal of Electroanalytical Chemistry 1996;404:37-43. https://doi.org/10.1016/0022-0728(95)04321-7.

[91] Cha D, Ahn JH, Kim HS, Kim Y. Effects of clamping force on the water transport and performance of a PEM (proton electrolyte membrane) fuel cell with relative humidity and current density. Energy 2015;93:1338-44. https://doi.org/10.1016/j.energy.2015.10.045.

[92] Bazylak A, Sinton D, Liu Z-S, Djilali N. Effect of compression on liquid water transport and microstructure of PEMFC gas diffusion layers. Journal of Power Sources 2007;163:784-92. https://doi.org/10.1016/j.jpowsour.2006.09.045.

[93] Ince UU, Markötter H, George MG, Liu H, Ge N, Lee J, et al. Effects of compression on water distribution in gas diffusion layer materials of PEMFC in a point injection device by means of synchrotron X-ray imaging. International Journal of Hydrogen Energy 2018;43:391-406. https://doi.org/10.1016/j.ijhydene.2017.11.047.

[94] Hartnig C, Manke I, Kuhn R, Kleinau S, Goebbels J, Banhart J. High-resolution in-plane investigation of the water evolution and transport in PEM fuel cells. Journal of Power Sources 2009;188:468-74. https://doi.org/10.1016/j.jpowsour.2008.12.023.

[95] Zenyuk IV, Parkinson DY, Hwang G, Weber AZ. Probing water distribution in compressed fuel-cell gas-diffusion layers using X-ray computed tomography. Electrochemistry Communications 2015;53:24-8. https://doi.org/10.1016/j.elecom.2015.02.005.

[96] Manke I, Hartnig Ch, Grünerbel M, Lehnert W, Kardjilov N, Haibel A, et al. Investigation of water evolution and transport in fuel cells with high resolution synchrotron x-ray radiography. Appl Phys Lett 2007;90:174105. https://doi.org/10.1063/1.2731440.

[97] Forner-Cuenca A, Biesdorf J, Manzi-Orezzoli V, Gubler L, Schmidt TJ, Boillat P. Advanced Water Management in PEFCs: Diffusion Layers with Patterned Wettability III. Operando Characterization with Neutron Imaging. J Electrochem Soc 2016;163:F1389. https://doi.org/10.1149/2.0891613jes.

[98] Mrozewski KJ. Diagnosis of mechanical tightening of a single polymer electrolyte membrane fuel cell (LT-PEM and HT-PEM) in aeronautical applications. PhD thesis supervisors: Christophe Turpin and Antoine Picot. Toulouse, INPT, 2019.

[99] Hottinen T, Himanen O, Karvonen S, Nitta I. Inhomogeneous compression of PEMFC gas diffusion layer: Part II. Modeling the effect. Journal of Power Sources 2007;171:113–21. https://doi.org/10.1016/j.jpowsour.2006.10.076.

[100] Carral C, Charvin N, Trouvé H, Mélé P. An experimental analysis of PEMFC stack assembly using strain gage sensors. International Journal of Hydrogen Energy 2014;39:4493-501. https://doi.org/10.1016/j.ijhydene.2014.01.033.

[101] Smart Solutions in Graphites & Fiber Composites. SGL Carbon. https://www.sglcarbon.com/en/.

[102] El-kharouf A, Mason TJ, Brett DJL, Pollet BG. Ex-situ characterisation of gas diffusion layers for proton exchange membrane fuel cells. Journal of Power Sources 2012;218:393-404. https://doi.org/10.1016/j.jpowsour.2012.06.099.

[103] Qiu D, Janßen H, Peng L, Irmscher P, Lai X, Lehnert W. Electrical resistance and microstructure of typical gas diffusion layers for proton exchange membrane fuel cell under compression. Applied Energy 2018;231:127-37. https://doi.org/10.1016/j.apenergy.2018.09.117.

[104] Barbir F. PEM Fuel Cells, Second Edition: Theory and Practice. 2 Edition. Amsterdam: Academic Press; 2012.

[105] Iranzo A, Boillat P. Liquid water distribution patterns featuring back-diffusion transport in a PEM fuel cell with neutron imaging. International Journal of Hydrogen Energy 2014;39:17240-5. https://doi.org/10.1016/j.ijhydene.2014.08.042.